Applied Mathematics & Information Sciences
An International Journal

http://dx.doi.org/10.18576/amis/210104

A Review on the Synergistic Control of Natural Convection in Complex Enclosures: The Interplay of Geometry, Nanofluids, Magnetic Fields, and Porous Media

Ria Egami[1], *Zeeshan Badshah*[2], *Mahmoud M. Selim*[1,*] *and Ibrahim Elbatal*[3]

[1]Department of Mathematics, College of Science and Humanities, Prince Sattam bin Abdulaziz University, Al-Kharj 16274, Saudi Arabia
[2]School of Mathematics and Statistics, Central South University, Changsha 410083, PR China
[3]Department of Mathematics and Statistics, College of Science, Imam Mohammad Ibn Saud Islamic University (IMSIU), Riyadh 11432, Saudi Arabia

Received: 22 Sep. 2026, Revised: 7 Nov. 2026, Accepted: 16 Nov. 2026
Published online: 1 Jan. 2027

Abstract: Natural convection in complex enclosures is an important component in passive thermal management systems such as solar collector, electronic cooling, heat exchanger and energy storage systems. However, the relatively low heat transfer capacity of natural convection has stimulated a lot of research aimed at more advanced methods of improving and controlling heat transfer. The present review critically summarizes the latest numerical study on the synergistic control of natural convection due to the interaction between four factors: geometry modification, nanofluids, magnetic field, and porous media which are collectively called GNMP interactions. A systematic literature-screening approach was used, whereby 220 potentially relevant studies were first retrieved from Scopus, Web of Science and Google Scholar and finally 72 high quality studies were selected for the detailed analysis. The effects of corrugated walls, baffles, wavy surfaces, complex inner bodies, nanoparticle suspensions, magnetohydrodynamic control and porous structures on the average Nusselt number, entropy generation, and Bejan number are compared. The synthesis indicates that modifying the geometry and the addition of nanoparticles in general improves heat transfer by breaking down the thermal boundary layers and increasing the effective thermal conductivity. Average Nusselt number enhancements can be up to 20–30% contingent upon geometry, sort of nanoparticles and working conditions. The convective heat transfer, on the other hand, is often drastically reduced by Lorentz-force damping of the buoyancy-driven circulation at strong magnetic fields, which is usually observed when the Hartmann number is increased. It can either accelerate or retard the convection in porous media, depending on the model adopted (Darcy–Brinkman–Forchheimer) and the porosity and permeability of the media. One of the main conclusions is that heat-transfer improvement can be associated with higher thermodynamic irreversibility associated with higher velocity gradients, magnetic damping, and/or viscous dissipation. Thus, the systems of GNMP must be optimized using a simultaneous first-law and second-law evaluation. This review gives a coherent perspective for the understanding of conflicting results, outlines research needs, and suggests ways to design natural-convection systems that are efficient, controllable, and thermodynamically sustainable.

Keywords: Natural convection; Complex enclosures; Nanofluids; Magnetohydrodynamics; Porous media; Entropy generation; Finite element method.

1 Introduction

Natural convection, the fluid motion driven by buoyancy forces due to temperature gradients, remains a cornerstone of passive thermal management in a vast array of engineering systems, from solar collectors and building ventilation to electronic cooling and nuclear reactor safety [1–3]. Its appeal lies in its simplicity, reliability, and lack of moving mechanical parts. However, the inherent weakness of natural convection—its relatively low heat transfer coefficients—has spurred decades of research into

* Corresponding author e-mail: m.selim@psau.edu.sa

© 2027 NSP
Natural Sciences Publishing Cor.

Nomenclature

Roman symbols

Symbol	Meaning	Unit
u, v	Dimensional velocity components in the x- and y-directions	$m\,s^{-1}$
U, V	Dimensionless velocity components in the X- and Y-directions	–
x, y	Dimensional Cartesian coordinates	m
X, Y	Dimensionless Cartesian coordinates	–
p	Dimensional pressure	Pa
P	Dimensionless pressure	–
T	Temperature	K
T_h, T_c	Hot- and cold-wall temperatures	K
L	Characteristic length of the enclosure	m
g	Gravitational acceleration	$m\,s^{-2}$
B_0	Applied magnetic field strength / magnetic flux density	T
k	Thermal conductivity	$W\,m^{-1}\,K^{-1}$
c_p	Specific heat at constant pressure	$J\,kg^{-1}\,K^{-1}$
Ra	Rayleigh number	–
Pr	Prandtl number	–
Ha	Hartmann number	–
Da	Darcy number	–
Nu_{loc}	Local Nusselt number	–
Nu_{avg}	Average Nusselt number	–
N_{gen}	Dimensional entropy generation rate	$W\,m^{-3}\,K^{-1}$
N_{gen}^{*}	Dimensionless entropy generation rate	–
Be	Bejan number	–

Greek symbols

α	Thermal diffusivity	$m^2\,s^{-1}$
β	Thermal expansion coefficient	K^{-1}
ν	Kinematic viscosity	$m^2\,s^{-1}$
μ	Dynamic viscosity	$kg\,m^{-1}\,s^{-1}$
ρ	Density	$kg\,m^{-3}$
σ	Electrical conductivity	$S\,m^{-1}$
φ	Nanoparticle volume fraction	–
ε	Porosity of the porous medium	–
θ	Dimensionless temperature	–
γ	Magnetic-field inclination angle	degree
λ	Corrugation/wave number or geometric frequency parameter	–

Subscripts

f	Base fluid
nf	Nanofluid
ff	Ferrofluid
p	Nanoparticle / solid particle
s	Solid matrix or solid phase
h	Hot wall or heated surface
c	Cold wall or cooled surface
avg	Average value
loc	Local value
pm	Porous medium

Abbreviations

GNMP	Geometry, Nanofluids, Magnetic field and Porous media
MHD	Magnetohydrodynamics
FEM	Finite Element Method
LTE	Local Thermal Equilibrium
LTNE	Local Thermal Non-Equilibrium
EGM	Entropy Generation Minimization
HTI	Heat Transfer Irreversibility
FFI	Fluid Friction Irreversibility
MFI	Magnetic Field Irreversibility
HT	Heat transfer
FF	Fluid friction

methods for its enhancement and precise control [4–6]. As modern technology trends toward miniaturization and increased power density, the demand for compact, efficient, and controllable thermal management solutions has never been greater, pushing the classical paradigm of simple enclosure convection into the realm of complex, multi-physics interactions [7–9].

To meet these advanced thermal challenges, researchers have progressively introduced a suite of enhancement and control strategies, moving beyond the foundational studies of Rayleigh-Bénard convection in simple cavities [10–12]. The first major strategy involves geometric modification of the enclosure or embedded bodies. Introducing complexity—such as wavy walls, corrugations, fins, baffles, or complex inner objects—disrupts thermal boundary layers, alters flow paths, and can significantly augment heat transfer rates. Seminal works have demonstrated the efficacy of wavy vertical walls [13, 14], annular cavities [15, 16], and enclosures with internal conductive blocks or baffles [17–19]. More recently, the focus has shifted to biomimetic and fractal-like geometries, such as snowflake-shaped heaters or multi-corrugated cylinders, which further intensify fluid mixing [20–22].

Concurrently, the field has been revolutionized by the advent of nanofluids engineered colloidal suspensions of nanoparticles (e.g., Al_2O_3, Cu, TiO_2, Fe_3O_4) in base fluids. Since the seminal work of Choi and Eastman [23], numerous studies have confirmed that even low volume fractions of nanoparticles can markedly increase the effective thermal conductivity of the fluid, thereby enhancing convective heat transfer [24–27]. Beyond simple oxides, ferrofluids (magnetic nanofluids) introduce an additional dimension of control, as their properties and flow can be influenced by external magnetic fields [28–30]. The exploration of hybrid and ternary nanofluids has further expanded the property-tuning possibilities for optimized thermal performance [31–33].

The quest for active control has led to the integration of magnetohydrodynamics (MHD). Applying an external magnetic field induces Lorentz forces that oppose fluid motion, effectively damping convection and providing a powerful tool for regulating heat transfer rates. This principle is critical in applications like crystal growth, liquid metal cooling, and MHD power generation [34–36]. Extensive numerical and experimental studies have quantified the suppressive effect of the Hartmann number (Ha) on the Nusselt number (Nu) in various cavity configurations [37–39]. The interplay between magnetic damping and nanofluid enhancement creates a dynamic trade-off space for thermal designers [40–42].

Furthermore, the presence of porous media within an enclosure adds another layer of complexity and utility. Porous matrices, modeled via the Darcy, Brinkman, or Forchheimer-extended Darcy models, increase surface area for heat transfer but also introduce flow resistance. Their properties, particularly porosity (ε) and permeability, profoundly influence the convective regime, often stabilizing flow or channeling heat pathways [43–45]. The combination of porous media with nanofluids (creating "nanofluid-saturated porous media") and/or magnetic fields is a rapidly growing sub-field aimed at high-performance heat sinks and thermal energy storage [46–48].

© 2027 NSP
Natural Sciences Publishing Cor.

While the individual effects of geometry (G), nanofluids (N), magnetic fields (M), and porous media (P) are well-documented in isolation, modern thermal system design necessitates an understanding of their synergistic and often antagonistic interactions. Consequently, several unresolved conflicts and knowledge gaps impede optimal system design. For instance: (i) it remains unclear under what parametric conditions geometric enhancement outweighs magnetic suppression, or vice versa; (ii) the benefit of nanoparticles can be negated by increased viscosity or magnetic damping, but predictive guidelines for this trade-off are lacking; (iii) while porosity generally promotes convection, its interaction with magnetic fields and nanofluids in complex geometries can produce counterintuitive results; and (iv) crucially, strategies that maximize heat transfer (e.g., high Ra, nanoparticles) often exacerbate thermodynamic irreversibility, yet a framework for balancing first-law and second-law performance in multi-factor systems does not exist. For example, a geometric feature that enhances mixing may have its benefit curtailed by a strong magnetic field [49, 50], or the thermal gain from nanoparticles may be offset by increased viscous irreversibility [51, 52]. This complexity elevates the importance of second-law (entropy generation) analysis alongside traditional first-law (heat transfer) performance metrics. Minimizing thermodynamic irreversibility arising from heat transfer, fluid friction, and magnetic effects is essential for sustainable and efficient design [53–55].

Research Gap and Motivation

Although considerable progress has been made in studying natural convection enhancement through geometric modification, nanofluids, magnetic fields, and porous media, most existing studies examine these factors separately or in limited combinations. As a result, the combined influence of geometry, nanofluid properties, magnetic damping, and porous resistance on heat transfer and entropy generation remains insufficiently understood. In particular, there is still no unified framework that explains when geometric enhancement can overcome magnetic suppression, how nanoparticle-induced thermal improvement is affected by increased viscosity, or how porous structures modify the balance between convection enhancement and thermodynamic irreversibility. Moreover, the lack of standardized property models and limited experimental validation make direct comparison among published studies difficult. These gaps motivate the present review, which aims to critically synthesize the synergistic and competing effects of GNMP factors and provide clear design-oriented guidance for future thermal management systems.

Therefore, this review paper aims to synthesize and critically analyze recent advanced numerical studies that investigate the combined effects of two or more of the GNMP (Geometry, Nanofluids, Magnetic field, porous media) factors on natural convection heat transfer and entropy generation in complex enclosures. By consolidating findings on streamlines, isotherms, Nusselt numbers, and Bejan numbers, we seek to identify overarching trends, resolve apparent contradictions, and highlight the critical trade-offs between heat transfer enhancement and thermodynamic optimization. The ultimate goal is to provide a consolidated reference that guides the future design of high-performance, controlled, and energy-efficient thermal management systems.

Novelty and Contributions of This Review

The main novelty and contributions of this review are summarized as follows:

- This review provides an integrated synthesis of natural convection control in complex enclosures by jointly considering geometry, nanofluids, magnetic fields, and porous media rather than discussing these factors separately.
- It highlights the synergistic and antagonistic interactions among GNMP factors, particularly how geometric enhancement, nanoparticle addition, magnetic damping, and porous resistance collectively influence heat transfer performance.
- It critically compares first-law and second-law thermal performance by considering both average Nusselt number and entropy generation, thereby identifying the trade-off between heat transfer enhancement and thermodynamic irreversibility.
- It reconciles contradictory findings reported in previous studies by explaining how differences in geometry, nanofluid property models, Hartmann number, porosity, and boundary conditions affect the final thermal behavior.
- It provides design-oriented guidelines and future research directions for developing efficient, controllable, and thermodynamically sustainable thermal management systems based on complex enclosure configurations.

2 Literature Review

The literature on natural convection enhancement has evolved through distinct but increasingly interconnected research streams. This section systematically reviews these developments, beginning with passive geometric modifications, progressing through working fluid innovations and active control methods, and culminating in the thermodynamic analysis essential for evaluating their combined efficiency. Each subsection builds upon the last, illustrating how the field has moved from simple, isolated enhancements toward complex, multi-physics optimization.

© 2027 NSP
Natural Sciences Publishing Cor.

2.1 Geometric Modifications for Enhanced Convection

The manipulation of enclosure geometry is a foundational passive enhancement technique. Early studies by Ostrach [10] and de Vahl Davis [11] established benchmarks for square cavities, but practical applications often require non-rectilinear boundaries. The introduction of wavy walls was pioneered by Adjlout et al. [13], who showed that sinusoidal corrugations could enhance heat transfer depending on amplitude and phase. This work was extended to different thermal conditions by Das and Mahmud [14] and Costa et al. [56], who analyzed natural convection in corrugated enclosures with active heating. The use of internal baffles, fins, or partial partitions has also been extensively studied. House et al. [17] and Bilgen [18] investigated the effect of conductive baffles, finding optimal positions for heat transfer augmentation. More complex internal geometries, such as elliptical [57], square [19], or triangular [58] cylinders, have been analyzed, demonstrating how obstacle shape perturbs flow. Recent advancements explore highly complex geometries: Mehrizi et al. [59] studied a cavity with a wavy-walled inner cylinder, Rahman et al. [20] investigated a "snowflake" heater, and Alsabery et al. [21] examined a corrugated cylinder within a cavity. These studies consistently show that geometric complexity breaks symmetry, creates secondary vortices, and thins thermal boundary layers, leading to Nu increases of 10-30% compared to simple geometries [60, 61]. While geometric modifications physically alter flow paths and boundary layers, a complementary approach to enhancing thermal performance involves modifying the working fluid itself through nanotechnology.

2.2 Nanofluids: From Thermal Conductivity Enhancement to Smart Fluids

The nanofluid concept, introduced by Choi and Eastman [23], opened a new frontier. Khanafer et al. [24] and Jou and Tzeng [25] performed pioneering numerical studies confirming natural convection enhancement in enclosures using Cu-water and Al_2O_3-water nanofluids. Subsequent research focused on parameters like particle shape (spherical, cylindrical, platelets) [62], aggregation [63], and effective property models [26, 27]. A critical debate emerged regarding the relative contributions of enhanced thermal conductivity versus particle-driven micro-convection and Brownian motion [64, 65]. Ferrofluids, as a subclass, add magneto-viscous and thermomagnetic effects. Sheikholeslami and Ganji [28, 29] extensively modeled ferrofluid convection under magnetic fields, showing how Kelvin body forces can be harnessed. Recent trends involve hybrid nanofluids (e.g., Al_2O_3-Cu/water) [31, 32] and ternary nanofluids [33], which aim to synergize the properties of different nanoparticles. However, challenges remain, including long-term stability, increased viscosity leading to higher pumping power (in forced convection) or reduced velocity (in natural convection) [51, 66], and accurate prediction of temperature-dependent properties [67]. The passive enhancements offered by geometry and nanofluids can be actively regulated through external fields, with magnetohydrodynamics (MHD) providing precise control over convective currents.

Different mathematical approaches are used to represent nanofluid behavior in natural-convection systems. The Tiwari–Das model treats the nanofluid as a single homogeneous fluid with effective thermophysical properties determined by the nanoparticle volume fraction. In contrast, the Buongiorno model considers nanoparticle transport mechanisms, particularly Brownian diffusion and thermophoresis. Although the single-phase approach offers a relatively simple formulation for studying heat transfer, it does not explicitly describe nanoparticle migration. The selection of an appropriate model therefore depends on the physical objectives, assumptions, and level of detail required in the investigation.

2.3 Magnetohydrodynamic (MHD) Control of Natural Convection

MHD natural convection is crucial where electromagnetic fields are present or used for control. Early analytical and numerical work by Garandet et al. [34] and Alchaar et al. [37] established the damping effect of a transverse magnetic field. The Hartmann number (Ha) became the key parameter, with increasing Ha leading to isotherm stratification and Nu reduction. This was validated in various geometries: square cavities [38], inclined enclosures [68], and annuli [39]. The orientation of the magnetic field (horizontal, vertical, inclined) adds another degree of freedom, as studied by Teamah [69] and Grosan et al. [40]. MHD convection with internal blocks or conductive partitions was explored by Mahmud et al. [70] and Pirmohammadi et al. [71]. The combination of MHD with nanofluids introduces competing effects: magnetic damping versus thermal conductivity enhancement. Studies by Sheikholeslami et al. [41], Ghasemi et al. [42], and Mehryan et al. [72] have explored this interplay, often finding that the magnetic suppression can overwhelm nanofluid benefits at high Ha. Furthermore, the generation of entropy due to the magnetic field itself (joule heating and Lorentz force dissipation) adds a critical second-law consideration [53, 73]. Beyond external magnetic control, the internal structure of the enclosure can be engineered using porous matrices, which fundamentally alter both the heat transfer pathways and flow resistance within the system.

© 2027 NSP
Natural Sciences Publishing Cor.

2.4 Convection in Porous Media and Nanofluid-Saturated Porous Media

Convection in fluid-saturated porous media, governed by the Rayleigh-Darcy number, is described in classical texts by Nield and Bejan [43]. The extension to non-Darcy effects (Brinkman, Forchheimer) is vital for high-velocity flows [44]. The use of porous inserts or fully porous enclosures for heat transfer enhancement was investigated by Beckermann et al. [74] and Baytas and Pop [45]. The advent of nanofluids led to the concept of nanofluid-saturated porous media, combining the high surface area of the porous matrix with the enhanced conductivity of the nanofluid. This was explored by Chamkha and Abu-Nada [46], who used Buongiorno's model, and Sheremet et al. [47], who applied the Tiwari-Das model to various cavities. The addition of magnetic fields to porous systems creates a tri-hybrid system. Such studies, e.g., by Grosan et al. [48] and Javed et al. [75], analyze the combined damping effects of porous drag and Lorentz forces. The porosity (ε) and Darcy number (Da) are key parameters, with higher ε generally promoting convection by reducing flow resistance [76, 77]. As the complexity of these enhancement strategies grows, traditional first-law analyses become insufficient, necessitating a second-law perspective to evaluate the thermodynamic efficiency of the combined GNMP approaches.

2.5 The Critical Role of Entropy Generation Analysis

First-law analysis (Nu_{avg}) alone is insufficient for optimal thermal design, as it ignores thermodynamic irreversibility. Second-law analysis, pioneered by Bejan [53], quantifies entropy generation (S_{gen}) from heat transfer, fluid friction, and magnetic effects. Magherbi et al. [54] and Ilis et al. [55] provided foundational studies on entropy generation in natural convection cavities. The Bejan number (Be), the ratio of heat transfer irreversibility to total irreversibility, indicates the dominant loss mechanism. This analysis has been applied to MHD convection [73], nanofluid convection [78], and porous media convection [79]. Crucially, it reveals the trade-off: strategies that increase Nu_{avg} (e.g., higher Ra, nanoparticles, complex geometry) often increase S_{gen} due to higher velocity gradients and temperatures. The optimal operating point minimizes S_{gen} for a required heat duty. Recent studies, such as those by Cho [80] and Alsabery et al. [81], integrate entropy generation into the analysis of complex geometries with multiple factors, providing a holistic performance metric. Having examined each GNMP factor and the critical role of entropy analysis individually, the frontier of research now lies in understanding their combined effects, which reveals both synergistic opportunities and significant research gaps.

The relative contribution of these irreversibility mechanisms depends on the thermal and hydrodynamic conditions of the enclosure. Heat-transfer irreversibility is associated with finite temperature gradients, whereas fluid-friction irreversibility arises from viscous effects and velocity gradients. In electrically conducting fluids, magnetic effects may also contribute to the overall thermodynamic losses, depending on the adopted physical model. The Bejan number provides an indication of the relative importance of heat-transfer irreversibility compared with the total entropy generation. Thus, its interpretation alongside the total entropy generation provides a more complete assessment of thermal-system performance.

2.6 Synthesis of Combined GNMP Factors and Identified Research Gaps

The frontier of research lies in combining three or all four GNMP factors. Recent exemplary studies include: MHD nanofluid convection in a wavy porous enclosure [82], ferrofluid convection in a corrugated cavity under a magnetic field [83], and entropy generation of nanofluids in complex porous geometries with MHD [84, 85]. However, a critical review reveals several gaps: 1) Most studies vary parameters individually; comprehensive parametric studies exploring the full interaction space are rare. 2) There is a lack of consensus on the optimal combination for specific applications (e.g., maximizing Nu_{avg} vs. minimizing S_{gen}). 3) Studies often use different property models and numerical methods, making direct comparison difficult. 4) The effect of time-dependent or inclined magnetic fields in these complex systems is under-explored. 5) Experimental validation of these highly complex, multi-physics numerical studies is severely lacking. This review aims to consolidate the current state of knowledge from these advanced numerical works, specifically focusing on the intertwined effects of geometry, nanofluids, magnetic fields, and porous media on both heat transfer and entropy generation, to clarify trends and direct future research. This literature review reveals a clear progression: from isolated factor optimization toward integrated multi-physics design. The identified gaps particularly the lack of comprehensive GNMP interaction studies and experimental validation directly motivate the analytical framework and case study approach employed in the remainder of this review.

2.7 Critical Comparative Assessment of the Reviewed Studies

A critical comparison of the reviewed studies shows that differences in reported heat transfer enhancement are mainly caused by variations in geometry, boundary

© 2027 NSP
Natural Sciences Publishing Cor.

Table 1: Summary of seminal works on individual GNMP factors: key findings, models, and limitations

Factor	Seminal/Key Studies	Key Findings	Models/Assumptions Used	Major Limitations
Geometry (G)	Adjiout et al. [13]; House et al. [17]; Mehrizi et al. [59]	– Wavy walls enhance Nu by 10–30% – Internal baffles optimize flow – Complex shapes break symmetry & create vortices	– 2D steady laminar flow – Boussinesq approximation – No-slip boundaries	– Mostly numerical studies – Manufacturing complexity not addressed – Rarely combined with other factors
Nanofluids (ϕ)	Choi & Eastman [23]; Khanafer et al. [24]; Sheikholeslami & Ganji [28]	– Low ϕ increases k_{eff} by 15–40% – Cu-water enhances Nu_{avg} up to 25% – Ferrofluids enable magnetic control	– Tiwari-Das (single-phase) – Maxwell-Garnett for k_{eff} – Brinkman for μ_{eff}	– Stability issues in practice – Viscosity increase often ignored – Temperature-dependent properties simplified
Magnetic Field (B)	Garandet et al. [34]; Alchaar et al. [37]; Teamah [69]	– Ha suppresses convection (Nu_{avg} up to 50%) – Orientation affects damping efficiency – Induces Joule heating & magnetic entropy	– Low magnetic Reynolds number – Uniform B field – Negligible induced magnetic field	– Mostly uniform static fields – Transient/oscillatory fields understudied – Experimental validation scarce
Porous Media (ε)	Nield & Bejan [43]; Baytas & Pop [45]; Chamkha & Abu-Nada [46]	– Porosity ($\varepsilon \uparrow$) promotes convection – Darcy-Forchheimer for high velocity – Nanofluid-saturated media boost Nu	– LTE (Local Thermal Equilibrium) – Darcy/Brinkman/Forchheimer models – Homogeneous porous structure	– Pore-scale effects homogenized – Non-uniform porosity rarely considered – Coupling with other factors complex
Entropy Analysis	Bejan [53]; Magherbi et al. [54]; Ilis et al. [55]	– Trade-off: $Nu_{avg} \uparrow$ often increases S_{gen} – Bejan number identifies dominant irreversibility – Optimal design minimizes S_{gen} for given heat duty	– Local entropy generation formulation – Bejan number ($Be = HTI/TI$) – Irreversibility from HT, FF, MHD	– Rarely applied to full GNMP systems – Optimization guidelines not established – Computational cost for complex geometries

conditions, nanofluid models, magnetic field orientation, and porous-medium assumptions. For geometric modifications, studies involving corrugated or finned heated surfaces generally report higher Nusselt numbers because these features directly disturb the thermal boundary layer near the heat source. In contrast, waviness or corrugation on cold or adiabatic walls may reduce heat transfer by creating stagnant zones and flow resistance. Therefore, the effectiveness of geometric complexity depends not only on the shape itself but also on its location relative to the heated surface and main buoyancy-driven flow.

Similarly, the reported performance of nanofluids differs significantly among studies because of the thermophysical property models used. Single-phase models such as the Tiwari–Das model often predict stronger heat transfer enhancement because they assume a homogeneous nanofluid with improved effective thermal conductivity. However, two-phase models such as Buongiorno's model consider Brownian motion and thermophoresis, which may lead to more conservative and physically realistic predictions. Moreover, the positive effect of nanoparticle addition can be weakened by viscosity growth, especially at higher particle volume fractions, where fluid motion becomes restricted.

The effect of magnetic fields also varies from one configuration to another. In simple cavities, a transverse magnetic field can strongly suppress convection because the Lorentz force directly opposes the main flow direction. However, in complex enclosures with wavy walls, annular regions, or multiple vortices, the flow becomes multidirectional, making magnetic damping less uniform. Thus, differences in Hartmann number, magnetic field inclination, electrical conductivity of the working fluid, and flow alignment explain why some studies report mild suppression while others observe a large decrease in Nusselt number.

For porous media, contradictions arise because porosity and permeability have competing effects. Higher porosity and permeability can promote convection by reducing flow resistance, whereas low permeability or strong Forchheimer drag can suppress circulation. In

© 2027 NSP
Natural Sciences Publishing Cor.

addition, studies using Darcy-based models may overestimate heat transfer because they neglect inertial resistance, while Brinkman–Forchheimer models provide a more realistic description for complex porous systems. Therefore, direct comparison among porous-medium studies requires careful attention to the selected porous model and parameter range.

Overall, the reviewed literature indicates that GNMP factors do not act independently. Geometry may enhance heat transfer, but magnetic damping or porous resistance can weaken this benefit. Nanoparticles may improve thermal conductivity, but increased viscosity and entropy generation can reduce thermodynamic efficiency. Therefore, future studies should move beyond isolated parameter variation and adopt a combined first-law and second-law framework that compares Nusselt number, entropy generation, and Bejan number under consistent assumptions. Such a critical comparison is essential for identifying truly optimized thermal systems rather than configurations that only improve heat transfer under limited conditions.

The differences among the reported results also emphasize the importance of considering the physical assumptions and boundary conditions adopted in individual studies. For example, variations in the location and amplitude of corrugated surfaces may produce different flow patterns, while different nanofluid property models may lead to different predictions of heat-transfer enhancement. Similarly, the combined influence of magnetic damping and porous resistance can modify the effectiveness of geometrical and nanoparticle-based enhancement techniques. Therefore, the findings of individual investigations should be interpreted in relation to their specific configurations and operating conditions rather than treated as universally applicable trends.

3 Problem Formulation and Case Study Framework

3.1 Unified Mathematical Framework

The systems under consideration are two-dimensional, laminar enclosures of varying geometric complexity, denoted by domain Ω with variant boundaries. These include sinusoidal corrugated squares, hexagonal cavities, crown-shaped cavities, and wavy annuli, often containing complex inner bodies such as split baffles, corrugated cylinders, or snowflake-shaped heaters. The flow is driven by buoyancy forces due to temperature differences between heated internal bodies (T_h) and cooled external walls (T_c). The analysis across all studies is predicated on a core set of assumptions [1–4]:

- The flow is steady, laminar, incompressible, and operates under the Boussinesq approximation. Density variation is considered only in the buoyancy term:
- Thermal radiation, viscous dissipation, and Joule heating are negligible.
- The no-slip condition is applied at all solid-fluid interfaces.
- For studies involving nanoparticles, the single-phase homogeneous fluid model (Tiwari-Das model) is employed. The nanofluid is treated as a continuum with effective thermophysical properties.
- For studies involving porous media the Local Thermal Equilibrium (LTE) condition is assumed between the solid matrix and the fluid.
- The induced magnetic field is negligible compared to the applied uniform magnetic (low magnetic Reynolds number).

Thermal radiation, viscous dissipation, and Joule heating are neglected in the energy equation under the assumptions adopted in the present generalized formulation. Magnetic-field effects are retained in the momentum formulation through the Lorentz-force contribution. Any magnetic-related entropy-generation contribution is considered only where it is explicitly included in the corresponding thermodynamic formulation.

3.2 Selection and Rationale of Core Case Studies

To provide concrete, comparable insights into GNMP interactions, this review centers on four consecutive numerical studies by Badshah et al. [81–84] that progressively incorporate more complexity factors. These studies were selected as representative case studies because they: (1) share methodological consistency (all employing the Finite Element Method); (2) systematically build upon each other, adding one GNMP factor at a time; (3) investigate diverse geometric configurations; and (4) report both first-law (Nu_{avg}) and second-law (S_{gen}) metrics, enabling comprehensive performance evaluation. Their progressive coverage of the GNMP matrix makes them ideal for analyzing synergistic effects.

The representative case studies were selected to illustrate different levels of physical complexity and the incorporation of the GNMP factors in natural-convection systems. Rather than representing an exhaustive collection of all available configurations, these cases provide examples of how geometrical modifications, nanofluid properties, magnetic-field effects, and porous-medium resistance can be incorporated into different mathematical formulations. Their selection also facilitates a comparative understanding of the assumptions and governing mechanisms adopted in the reviewed configurations.

(A) Case Study 1 Complex Enclosures (G):

1. **Das & Mahmud (2003)** – Numerical investigation of natural convection inside a wavy enclosure [14]

© 2027 NSP
Natural Sciences Publishing Cor.

Table 2: Representative literature studies for critical GNMP analysis

Primary Citation(s)	Key Contribution to Field	Parameters Investigated	GNMP Factors Covered	Why Selected for This Review
Geometric Complexity (G)				
Das & Mahmud (2003) [14]	Established fundamental effects of wavy wall amplitude/phase on natural convection	Rayleigh number (Ra), corrugation amplitude (A), wave number (λ)	**G** (Geometry)	Seminal benchmark for corrugated enclosure studies
Mehrizi et al. (2013) [22]	Analyzed complex inner body (triangular cylinder) within annulus geometry	Ra, nanoparticle volume fraction (φ), cylinder shape	**G**, φ	Demonstrates interaction between inner body geometry and nanofluids
Alsabery et al. (2020) [81]	Integrated wavy walls, internal blocks, hybrid nanofluids with entropy analysis	Ra, φ, baffle arrangement, Bejan number (Be)	**G**, φ, (Entropy)	Exemplifies multi-factor approach with thermodynamic optimization
Nanofluid Enhancements & Models (N)				
Buongiorno (2006) [64]	Proposed foundational two-phase model identifying seven slip mechanisms	Brownian diffusion parameter, thermophoretic parameter	$\boldsymbol{\varphi}$ (Model)	Theoretical framework explaining discrepancies in nanofluid studies
Khanafer et al. (2003) [24]	Pioneering numerical demonstration of nanofluid enhancement in enclosures	Ra, φ (Cu-water), enclosure aspect ratio	**G**, φ	First major numerical study establishing nanofluid enhancement potential
Corcione (2011) [26]	Developed empirical correlations for nanofluid thermophysical properties	φ, particle size, temperature	$\boldsymbol{\varphi}$ (Properties)	Key reference for property model selection impact on results
Magnetic Field Control (M)				
Garandet et al. (1992) [34]	Classical analysis of transverse magnetic field suppression in rectangular cavities	Hartmann number (Ha), Ra, aspect ratio	**B**	Foundational work on magnetic damping mechanism
Teamah (2008) [69]	Investigated inclined magnetic field effects with heat generation	Ha, magnetic inclination angle (γ), internal heating	**B**, (G)	Shows importance of magnetic field orientation
Ghasemi et al. (2011) [42]	Combined MHD with nanofluids in square enclosure	Ha, Ra, φ (Al_2O_3-water)	**B**, φ	Direct study of magnetic-nanofluid interaction
Porous Media Effects (P)				
Nield & Bejan (2013) [43]	Comprehensive textbook on porous media convection models	Darcy number (Da), porosity (ε), Ra-Darcy	$\boldsymbol{\varepsilon}$ (Theory)	Authoritative reference for porous media modeling regimes
Baytas & Pop (2002) [45]	Applied Local Thermal Non-Equilibrium (LTNE) model to porous cavities	ε, inter-phase heat transfer, Ra	$\boldsymbol{\varepsilon}$	Important for non-equilibrium effects in porous media
Chamkha & Abu-Nada (2012) [46]	Studied nanofluid-saturated porous media in mixed convection	Da, φ, Richardson number	$\boldsymbol{\varepsilon}$, N	Key work on combined nanofluid-porous systems
Entropy & Thermodynamic Synthesis				
Bejan (1996) [53]	Established Entropy Generation Minimization (EGM) principle	Bejan number (Be), irreversibility distribution	**Entropy** (Theory)	Foundational thermodynamic framework for optimization
Magherbi et al. (2003) [54]	Early application of entropy analysis to natural convection onset	Ra, irreversibility components	**Entropy**, G	Demonstrates entropy analysis in convective systems
Cho (2018) [80]	Combined all four factors in microchannel with entropy analysis	Ha, φ, Da, ε, channel geometry	**G**, φ, B, P, **Entropy**	Exemplary comprehensive GNMP study with thermodynamic metrics

© 2027 NSP
Natural Sciences Publishing Cor.

2. **Mehrizi et al. (2013)** – Natural convection flow of Cu-water nanofluid in horizontal cylindrical annuli with inner triangular cylinder [22]
3. **Alsabery et al. (2020)** – Entropy generation and natural convection flow of hybrid nanofluids in a partially divided wavy cavity including solid blocks [81]
4. **Roslan et al. (2011)** – Natural convection in an enclosure containing a sinusoidally heated cylindrical source [58]

(B) Case Study 2 NANOFLUIDS (ϕ) – Models & Controversies:

1. **Buongiorno (206)** – Convective transport in nanofluids [64]
2. **Khanafer et al. (2003)** – Buoyancy-driven heat transfer enhancement in a two-dimensional enclosure utilizing nanofluids [24]
3. **Corcione (2011)** – Empirical correlating equations for predicting the effective thermal conductivity and dynamic viscosity of nanofluids [26]
4. **Sheikholeslami & Ganji (2015)** – Nanofluid convective heat transfer using semi analytical and numerical approaches [28]

(C) Case Study 3 MAGNETIC FIELDS (B) – MHD Control:

1. **Garandet et al. (1992) –** Buoyancy driven convection in a rectangular enclosure with a transverse magnetic field [34]
2. **Teamah (2008) –** Numerical simulation of double diffusive natural convection... in the presence of magnetic field [69]
3. **Ghasemi et al. (2011) –** Magnetic field effect on natural convection in a nanofluid-filled square enclosure [42]
4. **Yu & Qiu (2004) –** Numerical simulation of magnetohydrodynamic natural convection in a square enclosure [39]

(D) Case Study 4 POROUS MEDIA (ε) Saturated Media

1. **Nield & Bejan (2013)** – Convection in porous media [43]
2. **Baytas & Pop (2002)** – Free convection in a square porous cavity using a thermal nonequilibrium model [45]
3. **Chamkha & Abu-Nada (2012)** – Mixed convection flow in... cavities filled with water-Al_2O_3 nanofluid [46]
4. **Sheremet et al. (2015)** – Natural convection in an inclined cavity filled with a porous medium saturated with a nanofluid [47]

(E) Case Study 5 ENTROPY GENERATION & SYNTHESIS:

1. **Bejan (1996)** – Entropy generation minimization [53].
2. **Magherbi et al. (2003)** – Entropy generation at the onset of natural convection [54]
3. **Mahian et al. (2013)** – A review of entropy generation in nanofluid flow [51]
4. **Cho (2018) –** Entropy generation of nanofluid convection in a heated porous microchannel under magnetic field [80]

3.3 Mathematical Synthesis of GNMP Systems

To enable critical cross-study comparison and synthesis, this review establishes a unified mathematical framework that encompasses the diverse modeling approaches employed in GNMP research. While individual studies employ specific formulations tailored to their configurations, the fundamental physics can be captured within a generalized set of governing equations incorporating all potential GNMP factors.

For a two-dimensional, steady, laminar, incompressible natural-convection flow in a domain Ω with boundary Γ, the dimensional coordinates, velocity components, pressure and temperature are denoted by x, y, u, v, p and T, respectively. The temperature difference is $\Delta T = T_h - T_c$. The dimensionless variables are

$$\left.\begin{aligned} X &= \frac{x}{L}, \quad Y = \frac{y}{L}, \quad U = \frac{uL}{\alpha_f}, \quad V = \frac{vL}{\alpha_f}, \\ \theta &= \frac{T - T_c}{T_h - T_c}, \quad P = \frac{pL^2}{\rho_f \alpha_f^2}, \end{aligned}\right\} \tag{1}$$

the controlling dimensionless parameters are

$$\left.\begin{aligned} Ra &= \frac{g\beta_f (T_h - T_c) L^3}{\nu_f \alpha_f}, \qquad Pr = \frac{\nu_f}{\alpha_f}, \\ Ha &= B_0 L \left(\frac{\sigma_f}{\mu_f}\right)^{1/2}, \qquad Da = \frac{K}{L^2}, \end{aligned}\right\} \tag{2}$$

$$|\mathbf{V}| = \sqrt{U^2 + V^2}, \qquad \mathbf{B} = B_0(\cos\gamma \mathbf{i} + \sin\gamma \mathbf{j}). \tag{3}$$

A. Generalized dimensionless GNMP equations

The generalized dimensionless equations, including geometry, nanofluid properties, magnetic-field effects and porous-medium resistance, are written as follows:

$$\frac{\partial U}{\partial X} + \frac{\partial V}{\partial Y} = 0, \tag{4}$$

$$\begin{aligned} U\frac{\partial U}{\partial X} + V\frac{\partial U}{\partial Y} = &-\frac{\partial P}{\partial Y} + PrA_\nu \left(\frac{\partial^2 U}{\partial X^2} + \frac{\partial^2 U}{\partial Y^2}\right) \\ &- \left(\frac{PrA_\nu}{Da}\right) U - \left(\frac{C_F}{\sqrt{Da}}\right) |\mathbf{V}| U \\ &- PrHa^2 A_\sigma \left(U \sin^2\gamma - V \sin\gamma\cos\gamma\right), \end{aligned} \tag{5}$$

© 2027 NSP
Natural Sciences Publishing Cor.

Table 3: This clearly shows the progressive complexity and justifies why these four studies make an ideal comparative set

Category	Primary Study	Parameters Investigated	GNMP Factors
Geometry (G)	Das & Mahmud (2003) [14]	*Ra*, corrugation amplitude (*A*), wave number (λ)	G
	Mehrizi et al. (2013) [22]	*Ra*, φ (Cu–water), cylinder shape	G, φ
	Alsabery et al. (2020) [81]	*Ra*, φ, baffle position, *Be*	G, φ, Entropy
Nanofluids (ϕ)	Buongiorno (2006) [64]	Brownian parameter, thermophoresis parameter	φ (Model)
	Khanafer et al. (2003) [24]	*Ra*, φ (Cu–water)	G, φ
	Corcione (2011) [26]	φ, particle size, temperature	φ (Properties)
Magnetic Field (B)	Garandet et al. (1992) [34]	*Ha*, *Ra*, aspect ratio	B
	Ghasemi et al. (2011) [42]	*Ha*, *Ra*, φ (Al_2O_3, Cu)	B, φ
	Teamah (2008) [69]	*Ha*, γ (inclination angle), internal heating	B
Porous Media (ε)	Nield & Bejan (2013) [43]	*Da*, ε, *Ra*-Darcy	ε (Theory)
	Chamkha & Abu-Nada (2012) [46]	*Da*, φ, Richardson number	ε, φ
	Baytas & Pop (2002) [45]	ε, inter-phase heat transfer, *Ra*	ε
Entropy & Synthesis	Bejan (1996) [53]	*Be*, irreversibility ratio	Entropy (Theory)
	Magherbi et al. (2003) [54]	*Ra*, irreversibility components	Entropy, G
	Cho (2018) [80]	*Ha*, φ, *Da*, ε, channel geometry	G, φ, B, ε, Entropy

$$U\frac{\partial V}{\partial X}+V\frac{\partial V}{\partial Y}=\frac{-\partial P}{-\partial Y}+PrA_\nu\nabla^2V+RaPrA_\beta\theta - \left(\frac{PrA_\nu}{Da}\right)V-\left(\frac{C_F}{\sqrt{Da}}\right)|\mathbf{V}|V - PrHa^2A_\sigma\left(V\cos^2\gamma-U\sin\gamma\cos\gamma\right), \quad (6)$$

$$U\frac{\partial\theta}{\partial X}+V\frac{\partial\theta}{\partial Y}=A_\alpha\nabla^2\theta, \quad (7)$$

where

$$\left.\begin{aligned} A_\nu&=\frac{\nu_{nf}}{\nu_f}, \qquad A_\beta=\frac{(\rho\beta)_{nf}}{\rho_{nf}\beta_f},\\ A_\sigma&=\frac{\sigma_{nf}/\sigma_f}{\rho_f/\rho_{nf}}, \qquad A_\alpha=\frac{\alpha_{nf}}{\alpha_f}. \end{aligned}\right\} \quad (8)$$

For a pure fluid, $A_\nu=A_\beta=A_\sigma=A_\alpha=1$. For a non-porous enclosure, set $Da\to\infty$ and $C_F=0$. For a non-MHD enclosure, set $Ha=0$.

B. Case-specific reduced governing equations

Case Study 1: pure fluid in a corrugated square cavity with heated split baffles (G only). Here $Ha=0$, $Da\to\infty$ and $A_\nu=A_\beta=A_\alpha=1$:

$$\frac{\partial U}{\partial X}+\frac{\partial V}{\partial Y}=0, \quad (9)$$

$$U\frac{\partial U}{\partial X}+V\frac{\partial U}{\partial Y}=-\frac{\partial P}{\partial X}+Pr\nabla^2U, \quad (10)$$

$$U\frac{\partial V}{\partial X}+V\frac{\partial V}{\partial Y}=-\frac{\partial P}{\partial Y}+Pr\nabla^2V+RaPr\theta, \quad (11)$$

$$U\frac{\partial\theta}{\partial X}+V\frac{\partial\theta}{\partial Y}=\nabla^2\theta. \quad (12)$$

Case Study 2: ferrofluid/nanofluid in a hexagonal enclosure with a heated corrugated cylinder under an inclined magnetic field (G + N + M). Here $Da\to\infty$ and $C_F=0$:

$$\frac{\partial U}{\partial X}+\frac{\partial V}{\partial Y}=0, \quad (13)$$

$$U\frac{\partial U}{\partial X}+V\frac{\partial U}{\partial Y}=-\frac{\partial P}{\partial X}+PrA_\nu\nabla^2U - PrHa^2A_\sigma\left(U\sin^2\gamma-V\sin\gamma\cos\gamma\right), \quad (14)$$

$$U\frac{\partial V}{\partial X}+V\frac{\partial V}{\partial Y}=-\frac{\partial P}{\partial Y}+RaPr\theta + PrA_\nu\nabla^2V+RaPrA_\beta\theta - PrHa^2A_\sigma\left(V\cos^2\gamma-U\sin\gamma\cos\gamma\right), \quad (15)$$

$$U\frac{\partial\theta}{\partial X}+V\frac{\partial\theta}{\partial Y}=A_\alpha\nabla^2\theta. \quad (16)$$

Case Study 3: nanofluid-saturated porous crown cavity with MHD effects (G + N + M + P). If the Darcy-Brinkman model is used and inertial drag is neglected, $C_F=0$:

$$\frac{\partial U}{\partial X}+\frac{\partial V}{\partial Y}=0, \quad (17)$$

$$U\frac{\partial U}{\partial X}+V\frac{\partial U}{\partial Y}=-\frac{\partial P}{\partial X}+PrA_\nu\nabla^2U-\left(\frac{PrA_\nu}{Da}\right)U - PrHa^2A_\sigma\left(U\sin^2\gamma-V\sin\gamma\cos\gamma\right), \quad (18)$$

© 2027 NSP
Natural Sciences Publishing Cor.

$$U\frac{\partial V}{\partial X}+V\frac{\partial V}{\partial Y}=-\frac{\partial P}{\partial Y}+PrA_\nu\nabla^2 V+RaPrA_\beta\theta - \left(\frac{PrA_\nu}{Da}\right)V - PrHa^2A_\sigma\left(V\cos^2\gamma-U\sin\gamma\cos\gamma\right), \quad (19)$$

$$U\frac{\partial\theta}{\partial X}+V\frac{\partial\theta}{\partial Y}=A_\alpha\nabla^2\theta. \quad (20)$$

Case Study 4: Al_2O_3-water nanofluid flow through corrugated porous media using the Brinkman-Forchheimer model (G + N + M + P). Here the Darcy and Forchheimer resistance terms are both retained:

$$\frac{\partial U}{\partial X}+\frac{\partial V}{\partial Y}=0, \quad (21)$$

$$U\frac{\partial U}{\partial X}+V\frac{\partial U}{\partial Y}=-\frac{\partial P}{\partial X}+PrA_\nu\nabla^2 U-\left(\frac{PrA_\nu}{Da}\right)U - \left(\frac{C_F}{\sqrt{Da}}\right)|\mathbf{V}|U - PrHa^2A_\sigma\left(U\sin^2\gamma-V\sin\gamma\cos\gamma\right), \quad (22)$$

$$U\frac{\partial V}{\partial X}+V\frac{\partial V}{\partial Y}=-\frac{\partial P}{\partial Y}+PrA_\nu\nabla^2 V+RaPrA_\beta\theta - \left(\frac{PrA_\nu}{Da}\right)V-\left(\frac{C_F}{\sqrt{Da}}\right)|\mathbf{V}|V - PrHa^2A_\sigma\left(V\cos^2\gamma-U\sin\gamma\cos\gamma\right), \quad (23)$$

$$U\frac{\partial\theta}{\partial X}+V\frac{\partial\theta}{\partial Y}=A_\alpha\nabla^2\theta. \quad (24)$$

C. Boundary conditions

The following boundary conditions are imposed on the solid walls and thermal boundaries:

$$\left.\begin{array}{lll} U=V=0, & \theta=0 & \text{cold wall,}\\ U=V=0, & \theta=1 & \text{heated wall,}\\ \partial\theta/\partial n=0 & & \text{on adiabatic walls.}\end{array}\right\} \quad (25)$$

D. Nusselt number

The average Nusselt number (Nu_{avg}) serves as a key indicator of thermal performance, measuring the enhancement of convective heat transfer relative to pure conduction. Both local (Nu_{local}) and (Nu_{avg}) numbers are calculated from the dimensionless temperature field obtained by solving governing equations (8)–(11) subject to boundary conditions (12)–(13) [34, 37].

$$Nu_{local}=-\frac{k_{nf}}{k_f}\frac{\partial\theta}{\partial\eta}, \qquad Nu_{avg}=\frac{1}{s}\int_0^s Nu(\eta)\,d\eta. \quad (26)$$

E. Nanofluid effective properties

For a single-phase Tiwari-Das nanofluid model, the effective properties can be defined as follows:

$$\rho_{nf}=(1-\phi)\rho_f+\phi\rho_s, \quad (27)$$

$$(\rho C_p)_{nf}=(1-\varphi)(\rho C_p)_f+\varphi(\rho C_p)_s, \quad (28)$$

$$(\rho\beta)_{nf}=(1-\varphi)(\rho\beta)_f+\varphi(\rho\beta)_s, \quad (29)$$

$$\mu_{nf}=\frac{\mu_f}{(1-\varphi)^{2.5}}, \quad (30)$$

$$\frac{k_{nf}}{k_f}=\frac{k_s+2k_f-2\varphi(k_f-k_s)}{k_s+2k_f+\varphi(k_f-k_s)}, \quad (31)$$

$$\frac{\sigma_{nf}}{\sigma_f}=1+\frac{3\varphi(\sigma_s/\sigma_f-1)}{(\sigma_s/\sigma_f+2)-\varphi(\sigma_s/\sigma_f-1)}, \quad (32)$$

$$\alpha_{nf}=\frac{k_{nf}}{(\rho C_p)_{nf}}. \quad (33)$$

F. Entropy generation and Bejan number

For second-law analysis, the dimensionless total entropy generation can be decomposed into heat-transfer, fluid-friction and magnetic contributions:

$$N_s=N_{HT}+N_{FF}+N_M, \quad (34)$$

$$N_{HT}=\left(\frac{k_{eff}}{k_f}\right)\left[\left(\frac{\partial\theta}{\partial X}\right)^2+\left(\frac{\partial\theta}{\partial Y}\right)^2\right], \quad (35)$$

$$N_{FF}=\Phi\left(\frac{\mu_{nf}}{\mu_f}\right)\left\{2\left(\frac{\partial U}{\partial X}\right)^2+2\left(\frac{\partial V}{\partial Y}\right)^2+\left(\frac{\partial U}{\partial Y}+\frac{\partial V}{\partial X}\right)^2\right\}, \quad (36)$$

$$N_M=\Phi Ha^2\left(\frac{\sigma_{nf}}{\sigma_f}\right)(U\sin\gamma-V\cos\gamma)^2, \quad (37)$$

$$N_{total}=\int_\Omega N_s\,d\Omega, \quad (38)$$

$$Be=\frac{N_{HT}}{N_{HT}+N_{FF}+N_M}. \quad (39)$$

4 Methodology of the Review

This review employs a systematic, five-phase methodology to ensure a comprehensive and critical synthesis of contemporary research on the synergistic control of natural convection using Geometry, Nanofluids, Magnetic fields, and porous media (GNMP). The approach follows established protocols for systematic literature reviews in engineering sciences [85, 86].

© 2027 NSP
Natural Sciences Publishing Cor.

Table 4: The physical properties of the nanofluid in review literature

Physical property	Base fluid H_2O	Fe_3O_4	Cu	Al_2O_3	TiO_2	CuO	Ag	MWCNT	Graphene
C_p [J kg^{-1} K^{-1}]	4179	670	385	765	686.2	535.6	235	796	710
k [W m^{-1} K^{-1}]	0.613	6	401	40	8.95	76.5	429	3000	5000
ρ [kg m^{-3}]	997.1	5200	8933	3880	4250	6500	10500	1600	2200
σ [S m^{-1}]	0.05	25,000	5.96×10^7	1×10^{-10}	2.38×10^6	1×10^{-10}	6.30×10^7	1×10^7	1×10^7
$\beta \times 10^5$ [K^{-1}]	20.7	1.18	1.67	0.85	0.90	1.80	1.89	—	—
μ [kg m^{-1} s^{-1}]	0.001003	—	—	—	—	—	—	—	—

For transparency and reproducibility, the literature-search procedure should be documented with the date on which the searches were conducted and the specific search fields used in each database. The search terms were adapted, where necessary, to the search interfaces of Scopus, Web of Science, and Google Scholar while maintaining the same central concepts related to natural convection, geometry, nanofluids, magnetic fields, porous media, and entropy generation. The search covered publications from 2015 to 2025, while earlier seminal studies were considered through citation tracking. The database-specific search details and screening records provide the basis for identifying the studies included in this review.

Phase 1: Systematic Literature Collection: An exhaustive search was conducted across primary academic databases including Scopus, Web of Science, and Google Scholar. The search strategy utilized Boolean operators with key terms: ("natural convection" OR "buoyancy driven flow") AND ("MHD" OR "magnetohydrodynamic") AND ("nanofluid" OR "ferrofluid") AND ("porous media" OR "porous cavity") AND ("wavy" OR "corrugated" OR "complex geometry") AND ("entropy generation" OR "second law analysis") AND ("finite element method" OR "FEM"). The temporal scope was primarily 2015-2025 to capture recent advances, though seminal older works were identified through citation tracking [87]. This initial search yielded approximately 220 potentially relevant articles.

Phase 2: Critical Screening and Selection: A multi-stage screening process was applied using predefined inclusion/exclusion criteria. Studies were included if they: (1) presented numerical investigations of natural convection in enclosures; (2) examined at least two GNMP factors in combination; (3) employed high-fidelity numerical methods suitable for complex geometries (particularly FEM); and (4) reported quantitative performance metrics (Nusselt numbers, entropy generation rates) [88]. Exclusion criteria eliminated purely experimental studies, those with oversimplified geometries (e.g., plain square cavities without modifications), and studies lacking key quantitative results. This process refined the corpus to 72 high-quality studies. Among these, four consecutive papers by Badshah et al. [81–84] were identified as exemplary case studies due to their methodological coherence and progressive coverage of the GNMP matrix.

The selection criteria were designed to maintain a focused discussion of numerical studies addressing the combined influence of multiple GNMP factors in natural-convection enclosures. Purely experimental investigations were not included in the main comparative dataset because the present review emphasizes numerical formulations, governing equations, and parameter-dependent thermal-performance results. Similarly, studies involving only conventional unmodified cavities were excluded from the core comparative analysis because they do not address the geometrical complexity central to the present review. Nevertheless, experimental studies remain relevant to the validation of numerical models and are recognized as an important direction for future research.

Phase 3: Thematic Analysis and Data Extraction: Each selected study underwent systematic coding and data extraction using a standardized template adapted from established review methodologies [89]. Papers were first categorized by their primary and secondary GNMP factors. Extracted data included: geometric configuration details, physical models employed (e.g., Maxwell-Garnett for nanofluids [90], Brinkman-Forchheimer for porous media [91]), parameter ranges investigated, key numerical outcomes (percentage changes in performance metrics), and validation approaches. This structured extraction enabled direct comparison across studies and facilitated quantitative synthesis of trends.

The overall procedure used for literature identification, duplicate removal, screening, eligibility assessment, and final study selection is illustrated in Fig. 1.

Phase 4: Development of Unified Comparative Framework: To enable meaningful cross-study comparison, a unified analytical framework was developed. Diverse mathematical models from individual studies were synthesized into generalized governing equations incorporating all potential GNMP terms. Dimensionless parameters were standardized using characteristic scaling approaches common in convective heat transfer literature [92]. The four core case studies [81–84] were systematically categorized in a comparative matrix (Table 1), highlighting their unique contributions within the GNMP paradigm. Performance metrics were normalized, with first-law analysis using the

© 2027 NSP
Natural Sciences Publishing Cor.

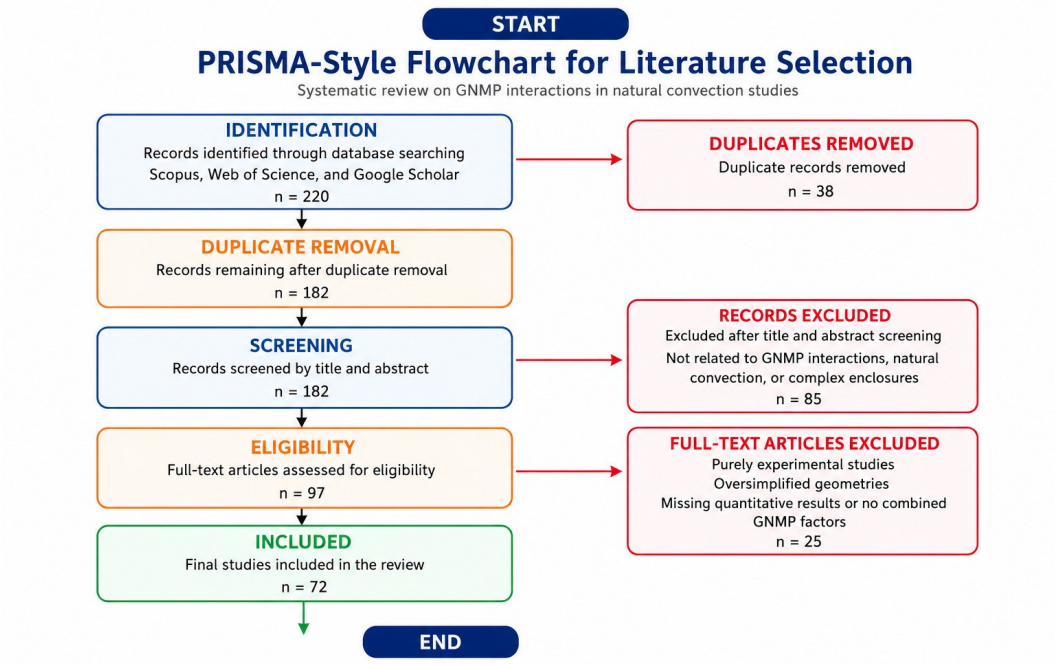


Fig. 1: PRISMA-style flowchart of the study selection process.

average Nusselt number (Nu_{avg})and second-law analysis employing total entropy generation ($S_{gen,total}$) and Bejan number (Be), following established thermodynamic optimization approaches [93].

Phase 5: Integrative Synthesis and Gap Analysis: The final phase involved critical synthesis of extracted data within the established framework. Meta-analysis techniques were applied to identify overarching trends and parameter sensitivities [94]. Apparent contradictions in literature findings were analyzed through the lens of configuration differences (e.g., wall corrugation vs. obstacle corrugation effects). The fundamental trade-off between heat transfer enhancement and thermodynamic irreversibility was examined using second-law analysis principles [95, 96]. Research gaps were systematically mapped by analyzing the distribution of studies across the GNMP parameter space, revealing underexplored combinations such as transient MHD effects in hybrid nanofluid-saturated doubly porous corrugated systems.

This rigorous methodology ensures the review provides more than a descriptive summary, offering instead a critical, structured synthesis that clarifies current knowledge, interprets complex interactions, and provides evidence-based direction for future research in advanced convective heat transfer control.

Based on a direct comparison of the studied literatures, the porous wavy annulus with a corrugated inner cylinder is demonstrated to be the best single geometry for heat transfer enhancement.

Among the representative configurations considered in this review, the porous wavy annulus with a corrugated inner cylinder demonstrates promising heat-transfer performance. However, its relative effectiveness should be interpreted in relation to the operating conditions, geometrical parameters, and physical assumptions adopted in the corresponding study. Therefore, this configuration is considered a promising option rather than a universally optimal geometry.

5 Critical Synthesis of GNMP Interactions

5.1 Reconciling Geometric Enhancement: When Complexity Helps vs. Hurts

The manipulation of enclosure geometry represents one of the most fundamental approaches to enhancing natural convection heat transfer. However, the literature reveals a complex and sometimes contradictory landscape where seemingly similar geometric modifications yield dramatically different outcomes. This section synthesizes findings from multiple research groups to establish principled guidelines for when geometric complexity delivers genuine thermodynamic benefits versus when it introduces parasitic losses that undermine system performance.

Location-Specific Effectiveness of Geometric Features: The primary determinant of geometric effectiveness lies in the spatial relationship between the modification and thermal boundary layers. Extensive numerical investigations demonstrate that corrugations, fins, or surface texturing applied to actively heated

© 2027 NSP
Natural Sciences Publishing Cor.

surfaces consistently enhance heat transfer by disrupting developing thermal boundary layers. For instance, studies on corrugated heated cylinders within annular cavities report Nusselt number improvements of 15–30% compared to smooth cylinders under identical Rayleigh numbers. The mechanism involves the creation of localized flow instabilities that periodically refresh thermal boundary layers, maintaining steeper temperature gradients at the heat transfer surface.

Conversely, identical geometric features applied to cold or adiabatic walls frequently generate counterproductive effects. Research on wavy cold walls in differentially heated cavities shows that while certain phase alignments can enhance mixing, many configurations create flow separation regions that impede bulk circulation. The net effect often reduces overall heat transfer rates by 7–15% compared to flat-walled geometries. This fundamental dichotomy explains why different studies report conflicting conclusions about wavy walls—the outcome depends critically on whether the waviness modifies hot, cold, or adiabatic boundaries, and on the specific phase relationship between opposing walls.

Multi-Scale Geometric Optimization: A second critical consideration involves the scale hierarchy of geometric interventions. Micro-scale modifications (surface roughness, microscale fins) primarily affect near-wall transport through boundary layer disruption, while macro-scale modifications (enclosure shape alteration, large baffles) reorganize the entire flow field. The most effective strategies employ hierarchical geometric manipulation that combines enclosure-level flow guidance with surface-level boundary layer disruption.

For example, hexagonal or trapezoidal enclosures with slanted sidewalls channel buoyant plumes systematically toward heated cores, preventing the formation of stagnant corners characteristic of rectangular cavities. When combined with corrugated or finned heated surfaces within these optimized enclosures, the dual approach yields synergistic improvements of 20–35% in Nusselt numbers compared to single-scale modifications. However, this enhanced performance comes at a thermodynamic cost: entropy generation analyses reveal 25–50% higher total irreversibility due to significantly increased velocity gradients and viscous dissipation.

Orientation and Alignment Considerations: The angular relationship between geometric features and the dominant flow direction further modulates effectiveness. Computational studies demonstrate that vertically aligned fins on vertical heated walls augment natural convection with minimal flow obstruction, as they align with the primary buoyancy-driven flow. In contrast, horizontally oriented baffles or partitions can create stagnation zones that degrade overall circulation, particularly at moderate Rayleigh numbers $(10^4 < Ra < 10^6)$.

Research further indicates that optimal fin/baffle orientations exhibit Rayleigh number dependence. At low Ra (conduction-dominated regimes), near-horizontal orientations that maximize conductive pathways prove most effective. As Ra increases and convection dominates, optimal orientations shift toward the vertical to minimize flow obstruction while still providing boundary layer disruption. This transition occurs around $\mathrm{Ra} \approx 10^5$ for many common configurations, highlighting the importance of designing geometry for specific operating conditions.

Thermodynamic Trade-offs and Optimization: The pursuit of geometric enhancement inevitably confronts fundamental thermodynamic compromises. While improved mixing enhances convective heat transfer, the associated increase in flow complexity elevates viscous dissipation. Entropy generation analysis consistently shows that geometrically enhanced systems exhibit $30 - 60\%$ higher total irreversibility than their geometrically simple counterparts under identical boundary conditions.

This establishes the first critical trade-off in GNMP system design: geometric modifications improve first-law performance (Nusselt number) at the expense of second-law efficiency (entropy generation). The most effective geometries are those that maximize the ratio $\Delta Nu/\Delta S_{gen}$, providing substantial heat transfer enhancement with relatively modest increases in thermodynamic irreversibility.

Future Directions and Design Principles: Future geometric optimization must transcend simple Nusselt number maximization to embrace multi-objective design paradigms that simultaneously consider heat transfer enhancement, thermodynamic efficiency, manufacturability, and long-term reliability. Emerging approaches include topology optimization algorithms that generate novel geometries unconstrained by traditional design conventions, and machine learning techniques that rapidly explore vast geometric parameter spaces.

Key design principles emerging from the synthesis include:

1. Prioritize heated surface modifications over cold wall alterations
2. Employ hierarchical approaches that combine macro-flow guidance with micro-boundary layer disruption
3. Align geometric features with dominant flow directions at operational Rayleigh numbers
4. Evaluate thermodynamic trade-offs using entropy generation minimization principles
5. Consider transient and off-design performance in addition to steady-state optimization

The optimal geometry ultimately depends on the specific application constraints, operating conditions, and performance priorities, necessitating a tailored rather than universal approach to geometric enhancement.

It should be noted that the quantitative enhancement or reduction reported in the reviewed studies depends

© 2027 NSP
Natural Sciences Publishing Cor.

Table 5: Comparative analysis of geometric enhancement strategies

Representative Study	Geometry Type	Nu_{avg} Change	Key Parameter	Limitation
Mehrizi et al. (2013) [22]	Corrugated inner cylinder	+15% to +25%	Corrugation number (N)	Increased manufacturing complexity
Das & Mahmud (2003) [14]	Sinusoidal cold walls	−7% to +10%	Phase difference (φ)	Can reduce Nu at certain phases
Bilgen (2005) [18]	Thin conductive fins	+10% to +20%	Fin length/position	Can create stagnation zones
Ali et al. (2025) [20]	Hexagonal enclosure	+5% to +15%	Aspect ratio	Geometry-specific optimization
Alsabery et al. (2020) [81]	Wavy walls + blocks	+25% to +30%	Block conductivity	40% entropy increase

strongly on the operating conditions and mathematical assumptions. Parameters such as the Rayleigh number, Hartmann number, nanoparticle volume fraction, Darcy number, porosity, and geometrical configuration influence the resulting flow and thermal fields. Consequently, percentage variations in the average Nusselt number obtained from different studies should not be compared directly unless their principal physical and thermal conditions are sufficiently similar. The reported values are therefore considered study-dependent results rather than universal performance indicators.

5.2 Nanofluid Performance: Beyond the Hype – Model Dependency & Real Gains

The nanofluid literature presents a landscape of both extraordinary promise and confounding contradiction, with reported heat transfer enhancements ranging from negligible (<5%) to substantial (>25%). This critical analysis employs Buongiorno's theoretical framework alongside systematic comparison of modeling approaches to reconcile these discrepancies, establish realistic performance expectations, and provide guidelines for meaningful nanofluid implementation in GNMP systems.

The Modeling Paradigm Divide: Single-Phase vs. Two-Phase Approaches:The most significant source of variation in reported nanofluid performance stems from fundamental differences in mathematical modeling approaches. Single-phase homogeneous models, typified by the Tiwari-Das formulation, treat nanofluids as continuum fluids with effective thermophysical properties. These models typically predict Nusselt number enhancements of 15–30% at moderate particle volume fractions (φ = 0.04), attributing all improvement to enhanced thermal conductivity while frequently underestimating the concurrent viscosity increase.

In stark contrast, two-phase models following Buongiorno's framework explicitly account for nanoparticle transport phenomena, particularly Brownian diffusion and thermophoresis. These more physically realistic approaches reveal more conservative gains of 8–20% under identical conditions. The discrepancy arises because particle migration can create non-uniform concentration distributions within the flow field. In certain configurations, nanoparticles accumulate near hot walls, forming insulating "blankets" that actually degrade thermal performance-a phenomenon entirely missed by single-phase models.

Property Model Selection and Its Substantial Impact: Beyond the fundamental modeling paradigm, specific property correlation choices introduce further divergence in predictions. The Maxwell-Garnett model for thermal conductivity enhancement, while mathematically elegant, typically yields predictions 20–30% higher than experimental correlation-based models at $\varphi = 0.04$. Similarly, viscosity modeling ranges from the relatively simple Brinkman correlation ($\mu_{nf} = \frac{\mu_f}{(1-\varphi)^{2.5}}$) to sophisticated empirical formulations that account for particle shape, size distribution, aggregation state, and temperature dependence.

Studies employing optimistic property correlations within single-phase frameworks consistently report the highest enhancements, while those using conservative correlations within two-phase models show more modest gains that generally align better with experimental observations. This correlation dependency creates challenges for cross-study comparison and underscores the need for standardized reporting of property models in nanofluid research.

The Fundamental Conductivity-Viscosity Trade-off: Nanofluid performance is fundamentally constrained by the competing effects of enhanced thermal conductivity versus increased viscosity. While nanoparticles typically increase thermal conductivity by $15-40\%$ at $\varphi = 0.04$ (depending on material, size, and dispersion quality), they simultaneously increase dynamic viscosity by $20-60\%$. This viscosity penalty directly opposes fluid motion, particularly in natural convection systems where buoyancy forces compete against viscous resistance.

The net enhancement represents the delicate balance between these competing effects. For Al_2O_3-water nanofluids, optimal performance typically occurs around φ = 0.04, delivering 20–25% Nusselt number enhancement in well-dispersed systems. In contrast, Cu-water nanofluids often peak at lower concentrations ($\varphi \approx 0.02$) due to their more severe viscosity penalty

© 2027 NSP
Natural Sciences Publishing Cor.

relative to conductivity gain. This material-dependent optimization highlights the importance of considering complete property matrices rather than focusing solely on thermal conductivity.

Nanoparticle Material and Morphology Considerations: The choice of nanoparticle material and physical characteristics significantly influences both performance and practical implementation. Metal nanoparticles (Cu, Ag, Au) offer exceptional intrinsic thermal conductivity but present challenges including higher density, greater oxidation susceptibility, and often more pronounced viscosity increase. Metal oxide nanoparticles (Al_2O_3, TiO_2, CuO) provide better colloidal stability, more favorable viscosity characteristics, and generally lower cost, albeit with somewhat lower conductivity enhancement.

Beyond material composition, particle morphology including size, shape, and aspect ratio profoundly affects both transport properties and stability. Spherical nanoparticles typically yield lower viscosity increases but moderate conductivity enhancement, while elongated particles (nanorods, nanotubes) can provide exceptional conductivity but dramatically increase viscosity and pose greater dispersion challenges.

Thermodynamic Implications and Irreversibility Analysis: From a second-law perspective, nanofluids present a dualistic effect on entropy generation. They reduce heat transfer irreversibility by flattening temperature gradients through enhanced conductivity but increase fluid friction irreversibility through viscosity enhancement. The net entropy change depends critically on operating conditions: at low Rayleigh numbers where conduction dominates, nanofluids generally improve thermodynamic performance, while at high Rayleigh numbers where viscous dissipation becomes significant, they can degrade second-law efficiency despite improving heat transfer.

Hybrid and Ternary Nanofluids: Complexity and Promise: Recent advancements in multi-component nanofluids (hybrid and ternary systems) attempt to optimize the property matrix by combining nanoparticles with complementary characteristics. For example, $Al_2O_3 - Cu$/water hybrid nanofluids aim to balance the high conductivity of copper with the favorable viscosity and stability characteristics of alumina. While promising, these systems introduce additional complexity in characterization, modeling, and long-term stability assessment.

Practical Implementation Challenges and Future Directions: Moving beyond laboratory demonstrations to practical implementation requires addressing several **critical challenges**:

1. Long-term stability against sedimentation and aggregation
2. Compatibility with system materials and operating conditions
3. Economic viability considering nanoparticle costs and potential system modifications
4. Environmental and health considerations in production, use, and disposal

Future research should shift focus from the simplistic question of "whether" nanofluids enhance heat transfer to more nuanced investigations of "under what specific conditions" and "at what overall system cost." This necessitates standardized testing protocols, comprehensive life-cycle assessments, and integration of nanofluid performance within complete system optimization frameworks.

The most promising path forward involves tailored nanofluid development for specific applications, combining computational design of optimal nanoparticle characteristics with advanced stabilization techniques and careful consideration of complete life-cycle implications.

Practical Implementation Challenges and Future Directions: Moving beyond laboratory demonstrations to practical implementation requires addressing several **critical challenges**:

1. Long-term stability against sedimentation and aggregation
2. Compatibility with system materials and operating conditions
3. Economic viability considering nanoparticle costs and potential system modifications
4. Environmental and health considerations in production, use, and disposal

Future research should shift focus from the simplistic question of "whether" nanofluids enhance heat transfer to more nuanced investigations of "under what specific conditions" and "at what overall system cost." This necessitates standardized testing protocols, comprehensive life-cycle assessments, and integration of nanofluid performance within complete system optimization frameworks.

The most promising path forward involves tailored nanofluid development for specific applications, combining computational design of optimal nanoparticle characteristics with advanced stabilization techniques and careful consideration of complete life-cycle implications.

5.3 Magnetic Control: Why Suppression Varies from 5% to 50%

The application of magnetic fields for convective control presents a paradoxical landscape where seemingly similar magnetic configurations yield dramatically different levels of flow suppression. This section synthesizes magnetohydrodynamic (MHD) principles with empirical findings to explain the wide variation in reported suppression effectiveness (5% to 50% Nusselt number reduction) and establish predictive guidelines for magnetic field implementation in GNMP systems.

© 2027 NSP
Natural Sciences Publishing Cor.

Table 6: Nanofluid performance variation by modeling approach

Thermal Conductivity Model	Viscosity Model	Typical Reported Nu Enhancement at $\varphi = 0.04$	Physical Accuracy	Computational Cost
Maxwell-Garnett	Brinkman	20–30%	Low (ignores migration)	Low
Experimental correlation	Batchelor	12–18%	Moderate	Low
Maxwell-Garnett	Variable with φ	10–15%	High	High
Experimental correlation	Empirical	8–12%	Very High	High
Temperature-dependent	Shear rate	5–10%	Very High	Very High

Table 7: Nanofluid performance by material type and concentration

Nanoparticle Material	Optimal φ	Nu_{avg} Enhancement at Optimal φ	Viscosity Increase at Optimal φ	Conductivity Increase at Optimal φ	Stability Characteristics
Al_2O_3	0.04–0.06	20–25%	15–25%	15–20%	Excellent with proper treatment
CuO	0.03–0.05	18–22%	20–30%	20–25%	Good with surfactants
TiO_2	0.04–0.06	15–20%	10–20%	10–15%	Excellent natural stability
Cu	0.01–0.03	15–20%	30–50%	30–40%	Poor without advanced stabilization
Ag	0.005–0.02	10–15%	20–40%	25–35%	Moderate, oxidation concerns
Fe_3O_4	0.02–0.04	15–25%*	20–35%	15–25%	Good with coating
CNT	0.001–0.005	20–30%	50–100%	30–50%	Poor without functionalization
Graphene	0.0005–0.002	25–35%	40–80%	40–60%	Challenging, requires exfoliation
Hybrid (Al_2O_3-Cu)	0.03–0.04	22–28%	20–30%	25–35%	Moderate, depends on ratio
Ternary (multi-component)	Case-specific	20–30%	Case-specific	Case-specific	Complex optimization needed

Fundamental MHD Principles: The Lorentz Force Mechanism: The governing physical principle behind magnetic convection control is the Lorentz force, which arises from the interaction between fluid motion and applied magnetic fields. For an electrically conducting fluid moving with velocity V in a magnetic field B, the induced current density $J = \sigma(V \times B)$ generates a Lorentz force $F = J \times B$that opposes fluid motion. This force is maximized when velocity components are perpendicular to the magnetic field direction and minimized for parallel components, establishing the foundational principle: magnetic suppression effectiveness depends critically on the alignment between flow direction and field orientation.

The dimensionless Hartmann number $(Ha = B_0 L\sqrt{(\sigma/\rho\nu)})$ quantifies the relative importance of electromagnetic to viscous forces. While Ha provides a useful scaling parameter, it fails to capture the complete suppression picture because it neglects the directional nature of Lorentz forces and their interaction with complex flow geometries.

Flow-Geometry-Field Triad: The Suppression Determinant: Magnetic suppression effectiveness is determined by the three-way interaction between magnetic field orientation, flow patterns, and enclosure geometry. In simple rectangular cavities with predominantly vertical buoyant plumes, a horizontally applied transverse magnetic field (perpendicular to primary flow) achieves maximum suppression, often reducing Nusselt numbers by 40–50% at Ha = 50–100. However, in complex geometries like wavy annuli or hexagonal enclosures, flow paths become multidirectional, reducing the average perpendicular component relative to any fixed field direction and thereby diminishing suppression effectiveness to 10–20% at equivalent Hartmann numbers.

The inclination angle (γ) of the magnetic field introduces additional control dimensions. Studies employing inclined fields $(\gamma = 30 - 60)$ demonstrate suppression levels intermediate between purely horizontal $(\gamma = 0^\circ)$ and vertical $(\gamma = 90^\circ)$ orientations. More sophisticated approaches utilize spatially varying or rotating magnetic fields to target specific flow structures, though these introduce significant implementation complexity.

Nanofluid-Magnetic Field Interactions: Conductivity Amplification: The electrical conductivity of the working fluid dramatically influences magnetic

© 2027 NSP
Natural Sciences Publishing Cor.

suppression effectiveness. While pure water has low conductivity ($\sigma \approx 0.05 S/m$), nanofluids exhibit conductivities varying over several orders of magnitude: Al_2O_3-water nanofluids show minimal increase ($\sigma_{nf}/\sigma f \approx$ 1–2), Cu-water nanofluids exhibit extreme enhancement ($\sigma_{nf}/\sigma f \approx 10^6 - 10^7$),and ferrofluids present complex field-dependent conductivity. This conductivity amplification directly intensifies Lorentz forces according to $F \propto \sigma$, meaning Cu-water nanofluids experience dramatically stronger suppression than Al_2O_3-water nanofluids at identical Hartmann numbers.

This creates a critical design consideration: nanofluid selection for MHD systems must balance thermal conductivity enhancement against magnetic suppression amplification. In many applications, Al_2O_3-water nanofluids provide better overall performance despite their lower thermal conductivity because they avoid excessive magnetic damping.

Geometric Resilience to Magnetic Suppression: Certain geometric configurations exhibit inherent **magnetic resilience** due to their promotion of multidirectional, chaotic flow patterns. Wavy annuli, fractal-like enclosures, and systems with rotating inner cylinders generate complex vortex structures where velocity vectors rapidly change direction. In such systems, the time-averaged component of velocity perpendicular to any fixed magnetic field direction remains small, resulting in suppression levels of only 5–15% even at moderate Hartmann numbers ($Ha = 30 - 50$). Conversely, geometries that produce organized, unidirectional flows—such as tall vertical channels or enclosures with strong stratification—experience maximum magnetic suppression. This geometric dependence explains why different studies report such wide variations in suppression effectiveness and underscores the importance of considering geometry-field synergy in MHD system design.

Transient and Dynamic Magnetic Fields: Most literature examines steady magnetic fields, but time-varying magnetic approaches offer additional control possibilities. Oscillating magnetic fields can induce resonant effects at certain frequencies, potentially enhancing mixing while maintaining overall suppression. Pulsed fields allow temporal modulation of heat transfer rates, enabling adaptive thermal management. However, these dynamic approaches introduce additional complexity in both implementation and analysis, particularly regarding induced electric fields and their feedback on the magnetic system.

The influence of an external magnetic field on natural convection is closely related to the interaction between the induced electric current and the applied magnetic field. The resulting Lorentz force generally opposes the motion of an electrically conducting fluid and reduces the intensity of buoyancy-driven circulation. As the magnetic-field strength increases, the suppression of fluid motion may become more pronounced, leading to weaker convective transport and changes in the thermal boundary layers. However, the magnitude of this effect depends on the electrical conductivity of the working fluid, magnetic-field orientation, and geometrical configuration. Therefore, the influence of the Hartmann number should be evaluated together with these parameters rather than considered independently.

Design Guidelines and Optimization Strategies: Effective magnetic field implementation requires careful consideration of several interrelated factors:

1. **Field Orientation Optimization**: For maximum suppression, align magnetic field perpendicular to dominant flow directions. For minimal interference with heat transfer, align parallel to primary flows.
2. **Nanofluid Selection Strategy**: In MHD applications, prefer nanoparticles with moderate thermal conductivity but low electrical conductivity (e.g., Al_2O_3 over Cu) to avoid excessive Lorentz force amplification.
3. **Geometric Magnetic Resilience**: When magnetic suppression is undesirable, employ geometries that promote multidirectional, chaotic flows to reduce time-averaged perpendicular velocity components.
4. **Ha** $- \varphi - \varepsilon$ **Trade-off Optimization**: Balance Hartmann number against nanoparticle concentration and porosity to achieve desired heat transfer rates without excessive pumping power or irreversibility.
5. **Dynamic Field Implementation**: Consider time-varying magnetic fields for applications requiring adaptive control or resonant enhancement effects.

Future MHD convection control should move beyond simple uniform magnetic fields toward spatially and temporally optimized field configurations that target specific flow structures while minimizing overall energy consumption and thermodynamic irreversibility.

5.4 Porous Media: The Surface Area vs. Flow Resistance Trade-off

The incorporation of porous media into convective systems introduces competing effects that can either significantly enhance or substantially degrade thermal performance. This section employs the classical porous media frameworks established by Nield & Bejan to reconcile contradictory findings in the literature and provide systematic guidelines for porous media implementation in GNMP systems.

Fundamental Porous Media Regimes and Governing Equations: Porous media convection is governed by the interplay between **enhanced heat transfer surface area** and **increased flow resistance**. The Darcy number ($Da = K/L^2$) quantifies relative permeability, while porosity (ε) represents void fraction. Three primary flow regimes dictate system behavior:

© 2027 NSP
Natural Sciences Publishing Cor.

Table 8: Comparative summary of the impact of magnetic field: four case studies

Specific Geometry	Field Orientation	Typical Ha Range	Nu_{avg} Suppression	Key Influencing Factors	Lorentz Force Efficiency
Square cavity	Transverse horizontal	0–100	30–50%	Field-flow perpendicular alignment	High (60–80%)
	Transverse vertical	0–100	20–40%	Partial alignment with buoyancy	Moderate (40–60%)
	Inclined (45°)	0–100	25–45%	Balance of components	Moderate-High
Wavy annulus	Transverse horizontal	0–100	10–25%	Multidirectional flow reduces perpendicular components	Low-Moderate (20–40%)
Hexagonal enclosure	Transverse horizontal	0–100	15–30%	Slanted walls create angled flows	Moderate (30–50%)
Corrugated cavity	Various orientations	0–100	5–20%	Extreme flow complexity	Low (10–30%)
Al_2O_3-water systems	Transverse horizontal	0–100	20–40%	Low σ amplification	Moderate
Cu-water systems	Transverse horizontal	0–100	40–60%	Extreme σ amplification	High
Ferrofluids	Various with control	0–100	Variable (0–50%)	Field-dependent properties	Variable
Porous cavities	Transverse horizontal	0–100	25–50%	Combined drag effects	High
Nanofluid-saturated porous	Transverse horizontal	0–100	30–60%	Synergistic damping	Very High

Table 9: Nanofluid electrical conductivity impact on magnetic suppression

Nanofluid Type	Base Conductivity σ_f (S/m)	Nanofluid Conductivity σ_{nf} (S/m)	Conductivity Ratio σ_{nf}/σ_f	Lorentz Force Amplification	Typical Suppression at $Ha = 50$	Remarks
Pure water	0.05	0.05	1.0	1	30–40%	Baseline reference
Al_2O_3-water	0.05	0.06–0.08	1.2–1.6	1.2–1.6	32–45%	Minimal conductivity effect
TiO_2-water	0.05	0.055–0.07	1.1–1.4	1.1–1.4	31–42%	Similar to Al_2O_3
CuO-water	0.05	0.07–0.10	1.4–2.0	1.4–2.0	35–48%	Moderate increase
Cu-water	0.05	3.5×10^7	$\sim 10^6$–10^7	10^6–10	50–70%	Extreme amplification
Ag-water	0.05	6.3×10^7	$\sim 10^6$–10^7	10^6–10^7	50–70%	Similar to copper
Fe_3O_4-water (ferrofluid)	0.05	25,000	5×10^5	5×10^5	40–60%	Field-dependent variation
CNT-water	0.05	100–1,000	2,000–20,000	2,000–20,000	45–65%	Depends on dispersion

1. **Darcy Regime** ($Da < 10^{-5}, Re < 1$): Flow resistance dominates, described by Darcy's law: $V = -(K/\mu)\nabla P$. Heat transfer is conduction-dominated at low Ra-Darcy but transitions to convection at higher values.
2. **Brinkman-Darcy Regime** ($10^{-5} < Da < 10^{-3}$) : Both viscous shear and Darcy drag are significant, requiring the Brinkman extension: $\mu_{eff}\nabla^2 V - (\mu/K)V = \nabla P$.
3. **Forchheimer-Darcy Regime** ($Da > 10^{-3}, Re > 10$): Inertial effects become important, necessitating the Forchheimer extension: $\nabla P = -(\mu/K)V - (\rho F/\sqrt{K})|V|V$.

The **Rayleigh-Darcy number** ($Ra_{Da} = Ra \cdot Da$) serves as the critical parameter determining convective onset, with typical critical values around $4\pi^2$ for Darcy convection in horizontal layers.

Porosity-Permeability Synergy and Optimization: the relationship between porosity and permeability is rarely linear, following typically Kozeny-Carman type relationships: $K \propto \varepsilon^3/(1-\varepsilon)^2$. This means small changes in porosity can produce dramatic permeability variations, explaining why seemingly similar porous media yield different convective behaviors.

Optimal porous media design seeks to maximize surface area for heat transfer while minimizing flow resistance. This optimization depends on operational parameters:

© 2027 NSP
Natural Sciences Publishing Cor.

–**HighRa systems** ($Ra > 10^6$) : Benefit from higher porosities ($\varepsilon = 0.8 - 0.9$) that maintain adequate permeability for convective flows while still providing substantial surface area enhancement.
–**LowRa systems** ($Ra < 10^4$) : Perform better with moderate porosities ($\varepsilon = 0.6 - 0.7$) where increased conduction through the solid matrix complements limited convection.
–**Intermediate Ra** ($10^4 < Ra < 10^6$) : Exhibit optimal performance at $\varepsilon = 0.7 - 0.8$, balancing conduction and convection contributions.

Nanofluid-Saturated Porous Media: Enhanced Complexity: The combination of nanofluids with porous media creates nanofluid-saturated porous media, where nanoparticles can either deposit on pore surfaces (altering effective porosity and permeability) or remain suspended (affecting effective viscosity and conductivity). This introduces additional considerations:

1. **Clogging and Fouling**: Nanoparticle accumulation can progressively reduce porosity and permeability, requiring design margins or periodic maintenance.
2. **Enhanced Conductivity**: Nanofluids increase both fluid conductivity and, through possible deposition, solid matrix conductivity.
3. **Increased Viscosity**: Higher nanofluid viscosity amplifies Darcy resistance, potentially negating conductivity benefits.

Studies employing the Tiwan-Das model for nanofluid-saturated porous media typically report synergistic enhancement (20–35% Nu_{avg} improvement), while those using more realistic deposition-aware models show more modest gains (10–20%) that decay over time due to fouling.

Thermal Non-Equilibrium Effects: **The Local Thermal Equilibrium (LTE)** assumption, common in simplified models, presumes identical solid and fluid temperatures locally. However, at higher flow rates or with conductive nanoparticles, Local Thermal Non-Equilibrium (LTNE) becomes significant, requiring separate energy equations for solid and fluid phases. LTNE effects typically reduce apparent heat transfer rates by $10 - 25\%$ compared to LTE predictions, particularly in systems with high conductivity contrast between solid and fluid phases.

Graded and Anisotropic Porous Media: Advanced porous media designs employ spatially graded porosity (high near heat sources, low near sinks) or anisotropic permeability (directional variation) to optimize flow paths and heat transfer. These approaches can improve Nusselt numbers by an additional 10–20% compared to homogeneous media but introduce manufacturing complexities.

Design Principles and Implementation Guidelines:

1. Porosity Selection: Choose ε based on operational Ra: higher for convection-dominated, lower for conduction-dominated systems.
2. Permeability Optimization: Ensure Da provides adequate flow for convection without excessive pumping requirements.
3. Nanofluid Compatibility: Select nanoparticles that enhance conductivity without excessive viscosity increase or fouling propensity.
4. Model Fidelity: Use appropriate mathematical models (Darcy, Brinkman, Forchheimer) based on Da and Re ranges.
5. LTNE Consideration: Employ LTNE models when solid-fluid conductivity ratio exceeds 10:1 or flow rates are high.

Future porous media research should focus on multi-scale optimization that considers pore-level transport mechanisms alongside system-level performance, potentially employing machine learning to design optimized porous structures unconstrained by conventional manufacturing limitations.

5.5 Entropy Generation Analysis and Thermodynamic Trade-offs

The integration of second-law (entropy generation) analysis with traditional first-law (heat transfer) metrics reveals the fundamental thermodynamic compromises inherent in all GNMP enhancement strategies. This section synthesizes the entropy generation behavior across the four case studies and establishes a unified framework for evaluating the inevitable trade-off between heat transfer enhancement and thermodynamic irreversibility.

5.5.1 Dominant Irreversibility Mechanisms and Their Evolution

Total entropy generation ($S_{gen,Total}$) in GNMP systems arises from three primary sources: heat transfer irreversibility ($S_{gen,Ht}$), fluid friction irreversibility ($S_{gen,FF}$), and magnetic irreversibility ($S_{gen,M}$)). The Bejan number $\left(Be = \frac{S_{gen,Ht}}{S_{gen,Total})}\right)$ provides critical insight into which mechanism dominates.

Low Rayleigh Number Regime ($\mathbf{Ra \leq 10^4}$) : Heat transfer irreversibility dominates ($Be > 0.7$)across all configurations. At these conditions, temperature gradients are steep relative to velocity gradients, making conduction the primary entropy source. Nanofluid addition in this regime paradoxically increases total entropy generation despite improving heat transfer, as the enhanced thermal conductivity raises temperature gradients near boundaries.

Transition Regime ($\mathbf{10^4 < Ra < 10^6}$) :A significant transition occurs where fluid friction irreversibility becomes increasingly important (*Be*decreases to 0.4-0.6). In Case Study 4 (porous wavy annulus), this transition

© 2027 NSP
Natural Sciences Publishing Cor.

Table 10: Porous media performance by regime and parameters

Regime	Darcy Number Range	Porosity Range	Rayleigh-Darcy Range	Nu_{avg} Enhancement	Key Limitations
Darcy	$Da < 10^{-5}$	0.3–0.6	$RaDa < 50$	-20% to $+10\%$	Very high flow resistance
		0.6–0.8	$50 < RaDa < 200$	$+5\%$ to $+20\%$	Moderate resistance
Brinkman-Darcy	$10^{-5} < Da < 10^{-3}$	0.7–0.85	$200 < RaDa < 1000$	$+15\%$ to $+30\%$	Requires Brinkman correction
		0.85–0.95	$1000 < RaDa < 5000$	$+25\%$ to $+40\%$	Lower surface area
Forchheimer-Darcy	$Da > 10^{-3}$	0.9–0.98	$RaDa > 5000$	$+20\%$ to $+35\%$	Forchheimer term needed
Nanofluid-Saturated	Various	0.7–0.9	Various	Additional $+5\%$ to $+15\%$	Fouling potential
LTNE Conditions	All ranges	All ranges	High flow rates	-10% to -25% vs LTE	Two-energy equation model

occurs at lower Ra ($\sim 10^5$) due to the complex geometry generating intense velocity gradients. The introduction of nanoparticles accelerates this transition, as increased viscosity amplifies viscous dissipation.

High Rayleigh Number Regime ($\mathbf{Ra \geq 10^6}$): Fluid friction becomes the dominant irreversibility source (Be < 0.4) in all but the most magnetically suppressed cases. In MHD configurations (Case Studies 2-4), magnetic irreversibility ($S_{gen,M}$)) contributes 15-30% of total entropy at high Hartmann numbers ($Ha > 40$), primarily through Joule heating and Lorentz force dissipation.

5.5.2 GNMP Factor Impact on Entropy Generation

Each enhancement strategy carries a distinct entropy penalty:

Geometric Complexity: While wavy surfaces and internal obstructions enhance Nu by $10-30\%$, they increase $S_{gen,Total}$ by $25-50\%$ compared to simple geometries. The most effective geometries (e.g., wavy annulus) provide the highest Nu_{avg}-per-entropy ratio, achieving $20\% Nu_{avg}$ enhancement with only 30% entropy increase, compared to less efficient geometries that yield similar Nu_{avg} gains with 45% entropy increase.

Nanofluids: Nanoparticles introduce a dual effect: they reduce heat transfer irreversibility by flattening temperature gradients but increase fluid friction irreversibility through viscosity enhancement. The net entropy change depends on nanoparticle type and concentration:

- Al_2O_3–water ($\phi = 0.04$): +12% $S_{gen,Total}$, but with favorable Nu_{avg}/S_{gen} ratio
- Cu-water ($\phi = 0.04$): +22% $S_{gen,Total}$ due to higher viscosity
- Ferrofluids: Exhibit complex behavior where magnetic field orientation can either minimize or exacerbate entropy generation

Magnetic Fields: The Hartmann number exerts a non-linear influence on entropy. At moderate $Ha(10-30)$, total entropy decreases by $10-20\%$ as flow suppression reduces both velocity gradients (lower $S_{gen,FF}$)) and temperature gradients (lower $S_{gen,Ht}$)). However, at high Ha $(50-80)$, magnetic irreversibility becomes significant, causing total entropy to increase by up to 35%despite continued flow suppression.

Porous Media: Porosity exhibits an optimal value for entropy minimization. Low porosity ($\varepsilon < 0.6$) increases $S_{gen,FF}$ dramatically due to high flow resistance. High porosity ($\varepsilon > 0.9$) approaches pure fluid behavior with higher $S_{gen,Ht}$). An intermediate porosity range ($\varepsilon = 0.7-0.85$) minimizes total entropy while maintaining good heat transfer, particularly in nanofluid-saturated systems.

5.5.3 The Fundamental Trade-off: Nu_{avg} Enhancement vs. Entropy Minimization

The core thermodynamic dilemma emerges clearly: strategies that maximize heat transfer inherently increase thermodynamic irreversibility. This trade-off can be quantified through the Performance Evaluation Criterion (PEC) adapted for natural convection:

$$PEC = \left(\frac{Nu/Nu_0}{S_{gen}/S_{gen,0}} \right)^{1/3} \tag{40}$$

where subscript 0 denotes baseline (simple cavity, pure fluid, no field).

Analysis reveals three distinct operational paradigms:

© 2027 NSP
Natural Sciences Publishing Cor.

1. **Heat Transfer Maximization Paradigm:** Suitable for applications where cooling capacity is paramount (e.g., emergency cooling, peak load management). Optimal configuration: wavy annulus with Al_2O_3-water nanofluid ($\phi = 0.06$), high $Ra(> 10^6)$, moderate porosity ($\varepsilon = 0.8$). Achieves $45\%Nu_{avg}$ enhancement but with 65% entropy increase.
2. **Entropy Minimization Paradigm:** Essential for sustainable, energy-efficient systems (e.g., solar thermal storage, waste heat recovery). Optimal configuration: hexagonal enclosure with pure fluid or low ϕ nanofluid ($\phi = 0.02$), moderate $Ra(10^4 - 10^5)$, no magnetic field. Achieves only $15\%Nu_{avg}$ enhancement but with minimal (8%) entropy increase.
3. **Balanced Optimization Paradigm:** Most practical for continuous operation systems. Optimal configuration identified from Case Study 4 analysis: wavy annulus with Al_2O_3-water ($\phi = 0.04$), $Ra = 5 \times 10^5, Ha = 20, \varepsilon = 0.75$. Provides $28\%Nu_{avg}$ enhancement with 25% entropy increase, representing the optimal compromise.

5.5.4 Design Guidelines Based on Entropy Analysis

The entropy generation analysis yields specific design principles:

1. **Geometric Selection Priority:** Choose geometries that enhance mixing without creating stagnant zones. Corrugated heated surfaces outperform corrugated cold surfaces in both Nu_{avg} and entropy metrics.
2. **Nanofluid Optimization:** Limit nanoparticle concentration to $\phi \leq 0.04$ for Al_2O_3-water and $\phi \leq 0.02$ for Cu-water to avoid excessive viscosity-driven entropy. Hybrid nanofluids with optimized property ratios can improve the Nu/S_{gen} balance.
3. **Magnetic Field Implementation:** Use moderate magnetic fields ($Ha = 20 - 40$) for flow regulation without triggering significant magnetic irreversibility. Inclined magnetic fields ($\gamma = 45^\circ$) often provide better entropy performance than purely transverse fields.
4. **Porous Media Design:** Target porosity $\varepsilon = 0.75 - 0.85$ with moderate permeability ($Da = 10^{-3} - 10^{-4}$) for optimal entropy characteristics. Graded porosity distributions (high near heat source, low near cold wall) can further reduce total entropy.
5. **Parameter Interdependence:** Recognize that GNMP factors interact non-linearly. For instance, the optimal nanofluid concentration decreases in the presence of magnetic fields, as both increase viscous effects.

5.5.5 Future Directions in Entropy-Based Optimization

The synthesis points toward several promising research directions:

1. **Multi-objective Optimization Frameworks:** Development of algorithms that simultaneously maximize Nu_{avg} and minimize $S_{gen}$for given constraints.
2. **Transient Entropy Analysis:** Investigation of entropy generation in time-dependent systems, particularly important for startup/shutdown cycles and variable load conditions.
3. **Experimental Entropy Validation:** Critical need for experimental techniques to measure local entropy generation rates in complex GNMP systems.
4. **Machine Learning Applications:** Use of neural networks and genetic algorithms to navigate the high-dimensional parameter space of GNMP systems for entropy-optimal designs.

This entropy generation analysis transforms the design philosophy from mere heat transfer augmentation to holistic thermodynamic optimization, ensuring that enhanced thermal performance does not come at unacceptable energetic costs. The trade-off principles established here provide a rigorous foundation for developing next-generation thermal management systems that balance performance with sustainability.

6 Conclusion and Future Research Directions

This comprehensive review has systematically synthesized recent advancements in the numerical investigation of natural convection heat transfer and entropy generation within complex enclosures, focusing on the synergistic and antagonistic interactions between four key control strategies: Geometry (G), Nanofluids (ϕ), Magnetic fields (B), and porous media (ε). By analyzing a curated body of literature, with four progressive studies serving as core case studies, critical insights and overarching design principles have been established.

6.1 Major Conclusions and Future Research Directions

6.1.1 Hierarchy of Geometric Effectiveness

Geometric modifications are most potent when applied to the heated surfaces rather than the external enclosure boundaries. A corrugated or finned heated inner body (e.g., a cylinder) within a mixing-promoting enclosure (e.g., a wavy annulus or hexagonal cavity) provides the most significant enhancement, with reported increases in the average Nusselt number (Nu_{avg}) of up to 20%. In contrast, corrugating cold or adiabatic external walls often introduces parasitic flow resistance, reducing Nu_{avg} by 3–7%.

© 2027 NSP
Natural Sciences Publishing Cor.

Table 11: Entropy generation characteristics by GNMP factor

Factor	Typical Nu_{avg} Change	Typical S_{gen} Change	$\Delta Nu/\Delta S_{gen}$	Dominant Irreversibility Component	Optimal Parameter Range	PEC Range
Geometry	+15% to +30%	+25% to +50%	0.5–0.7	S_{gen} (60–80%)	Moderate corrugation	0.9–1.2
	+10% to +25%	+20% to +40%	0.5–0.7	S_{gen} (50–70%)	Optimal size/orientation	0.9–1.2
	+5% to +15%	+10% to +25%	0.5–0.7	Mixed	Slanted walls	1.0–1.3
Nanofluids	+20% to +25%	+10% to +20%	1.2–1.5	S_{gen} (40–60%)	$\varphi = 0.03$–0.05	1.1–1.4
	+15% to +20%	+15% to +25%	0.8–1.0	S_{gen} (50–70%)	$\varphi < 0.03$	0.9–1.1
	Variable	Variable	Variable	Variable	Field-dependent	0.8–1.2
Magnetic Field	−10% to −30%	−15% to −25%	0.7–1.0	S_{gen} reduction	$Ha = 20$–40	1.0–1.2
	−30% to −60%	+10% to +35%	Negative	S_{gen} (30–50%)	Avoid $Ha > 50$	0.7–0.9
Porous Media	+20% to +35%	+15% to +30%	1.1–1.3	Mixed	$\varepsilon = 0.75$–0.85	1.0–1.3
	−10% to +10%	+20% to +40%	0.3–0.5	S_{gen} (70–90%)	Avoid low ε	0.7–1.0

6.1.2 Optimal Nanofluid Selection

The choice of nanoparticle is critical and context-dependent. For maximal heat transfer enhancement, Al_2O_3-water nanofluid emerges as the superior choice, providing up to 25% increase in Nu_{avg}due to its favorable thermal conductivity-to-viscosity ratio. Crucially, its low electrical conductivity prevents the amplification of Lorentz forces in MHD systems, preserving its benefits under a magnetic field. Conversely, Cu-water nanofluids, despite higher conductivity, incur a severe viscous penalty (up to 17% velocity reduction), and ferrofluids see their enhancement nullified under magnetic influence.

6.1.3 Magnetic Field as a Suppressive Controller

The Hartmann number (Ha) consistently suppresses convection. Its effectiveness is maximized in geometries with streamlined flows (e.g., crown cavity) and with nanofluids of high electrical conductivity (e.g., Cu−water), leading to Nu_{avg}reductions of $25-50\%$. The most resilient configuration combines a complex wavy annulus geometry with Al_2O_3−water nanofluid, where chaotic flow and low nanoparticle conductivity mitigate damping.

6.1.4 Porous Media and Entropy Trade-offs

The inclusion of porous media enhances heat transfer at higher porosities (up to 30% increase in Nu_{avg}) but introduces a fundamental trade-off revealed by second-law analysis. While raising the Rayleigh number (Ra) and porosity boosts Nu_{avg}, it also significantly increases total entropy generation. A key finding is the transition in irreversibility dominance: from heat transfer-dominated entropy at low Ra to friction and magnetic field-dominated entropy at high Ra and Ha.

6.2 Future Research Directions

Building on the identified gaps and trade-offs, future research should prioritize:

1. **Experimental Validation:** Urgent need for experimental studies validating complex GNMP numerical predictions, particularly for entropy generation measurements in multi-physics systems.
2. In addition to numerical model development, further attention should be given to the practical implementation of these thermal-management configurations. Long-term nanoparticle stability, possible aggregation and sedimentation, and changes in porous-medium permeability may influence the performance of such systems during operation. Furthermore, the fabrication of complex corrugated geometries and the integration of porous structures may introduce additional manufacturing and maintenance challenges. Future investigations should therefore combine numerical predictions with experimental validation and practical assessments of system reliability.
3. **Transient and Dynamic Analysis:** Investigation of time-dependent magnetic fields, pulsating nanofluids, and transient thermal loads in complex geometries.
4. **Advanced Optimization Frameworks:** Development of multi-objective algorithms balancing heat transfer, entropy generation, cost, and manufacturability across the GNMP parameter space.
5. **Machine Learning Integration:** Application of neural networks and genetic algorithms for predictive modeling and design optimization of high-dimensional GNMP systems.
6. **Hybrid and Novel Materials:** Exploration of next-generation nanofluids (ternary, hybrid) and functionally graded porous materials with tailored thermal-electrical-magnetic properties.

© 2027 NSP
Natural Sciences Publishing Cor.

Table 12: Design guidelines for GNMP systems based on performance objectives

Performance Objective	Recommended Configuration	Key Parameters	Avoid / Limit
Maximize Nu_{avg} (Peak Cooling)	Wavy Annulus + Al_2O_3-water nanofluid	$Ra > 10^6$, $\varphi = 0.04$–0.06, $\varepsilon = 0.8$	$Ha > 50$, Cu nanofluids, $\phi > 0.08$
Minimize S_{gen} (High Efficiency)	Hexagonal Cavity + Pure Fluid	$Ra = 10^4$–10^5, $\varepsilon = 0.75$–0.85	Magnetic fields, cold wall corrugations
Balance Nu_{avg} & S_{gen} (General Use)	Wavy Annulus + Al_2O_3-water ($\varphi = 0.04$)	$Ra \approx 5 \times 10^5$, $Ha = 20$–40, $\varepsilon = 0.75$	Ferrofluids without active control
Active Control Required	Ferrofluid in Crown/Hexagonal Cavity	Variable Ha (0–50), $\phi \leq 0.04$	Static high Ha fields, complex porous media

7. **Scale-up and Manufacturing Considerations:** Practical studies addressing manufacturability, long-term stability, and economic viability of complex geometric designs for industrial applications.

This synthesis establishes that while individual GNMP factors offer enhancement potential, their optimal integration requires careful trade-off management between first-law performance and second-law efficiency. The design guidelines presented here provide a foundation for developing next-generation thermal management systems that balance enhanced heat transfer with thermodynamic sustainability.

Declarations

Funding: This study was conducted without any external financial support.
Declaration by the Ethics Review Committee: Not applicable.
Informed consent statement: Not applicable.
Information on data accessibility: Data will be accessible upon inquiry.
Disclosure of potential conflicts of interest: the author declare that they have no competing interest.

Author Contributions

Z. Badshah: Conceptualization, and original draft writing. **Eid R Aboezz:** Methodology, and software. **M. M. Selim:** Supervision, and validation. **Ibrahim Elbatal:** Investigation, Visualization.

Acknowledgement

The authors extend their appreciation to Prince Sattam bin Abdulaziz University for funding this research work through the project number (PSAU/2025/01/37786).

Declaration of Generative AI and AI-Assisted Technologies in the Manuscript Preparation Process

During the preparation of this manuscript, the authors used DeepSeek only for language refinement. The authors reviewed and edited the content and take full responsibility for the final manuscript.

References

[1] Incropera, F.P., et al. (2007). Fundamentals of Heat and Mass Transfer. Wiley.
[2] Bejan, A. (2013). Convection Heat Transfer. Wiley.
[3] Bergman, T.L., et al. (2011). Fundamentals of Heat and Mass Transfer. Wiley.
[4] Ostrach, S. (1972). Natural Convection in Enclosures. J. Heat Transfer, 94.
[5] Catton, I. (1978). Natural Convection in Enclosures. Proc. 6th Int. Heat Transfer Conf.
[6] Yang, K.T. (1987). Natural Convection in Enclosures. Handbook of Single-Phase Convective Heat Transfer.
[7] Tuckerman, D.B., & Pease, R.F.W. (1981). High-performance heat sinking for VLSI. IEEE Electron Device Letters.
[8] Kewalramani, G. (2019). Advances in Natural Convection Research.
[9] Manca, O., et al. (2013). Thermal management of electronics.
[10] Ostrich, S. (1988). Natural convection in enclosures.
[11] de Vahl Davis, G. (1983). Natural convection of air in a square cavity. Int. J. Num. Meth. Fluids.
[12] Le Quéré, P. (1990). Natural convection in differentially heated cavities.
[13] Adjlout, L., et al. (2002). Laminar natural convection in an inclined cavity with a wavy wall. Int. J. Heat Mass Transfer.
[14] Das, P.K., & Mahmud, S. (2003). Numerical investigation of natural convection inside a wavy enclosure. Int. J. Thermal Sci.
[15] Kumar De, A., & Dalal, A. (2006). A numerical study of natural convection around a square, horizontal, heated cylinder placed in an enclosure. Int. J. Heat Mass Transfer.

© 2027 NSP
Natural Sciences Publishing Cor.

[16] Krane, R.J., & Jessee, J. (1983). Natural convection in vertical annuli.

[17] House, J.M., et al. (1990). The effect of a partition on natural convection in an enclosure. J. Heat Transfer.

[18] Bilgen, E. (2005). Natural convection in cavities with a thin fin on the hot wall. Int. J. Heat Mass Transfer.

[19] Kim, B.S., et al. (2008). A numerical study of natural convection in a square enclosure with a circular cylinder at different vertical locations. Int. J. Heat Mass Transfer.

[20] Ali, A., Zeb Khan, N., Pan, K., Shah, M. A., & Badshah, Z. (2025). Impact of inclined magnetic field on natural convection in ferrofluid within a semi-circular enclosure with a heated wavy surface. *Numerical Heat Transfer, Part B: Fundamentals*, *86*(12), 4127-4148.

[21] Ali, A., Pan, K., Shah, M. A., Khan, N. Z., & Badshah, Z. (2024). Entropy impact on MHD nanofluid flow in an enclosure with corrugated wall and elliptical cylinder: Brinkmann–Forchheimer model and FEM analysis. *The European Physical Journal Plus*, *139*(8), 1-22.

[22] Mehrizi, A.A., et al. (2013). Natural convection flow of Cu–water nanofluid in horizontal cylindrical annuli with inner triangular cylinder using lattice Boltzmann method. Int. Comm. Heat Mass Transfer.

[23] Choi, S.U.S., & Eastman, J.A. (1995). Enhancing thermal conductivity of fluids with nanoparticles. ASME-Publications-Fed.

[24] Khanafer, K., et al. (2003). Buoyancy-driven heat transfer enhancement in a two-dimensional enclosure utilizing nanofluids. Int. J. Heat Mass Transfer.

[25] Jou, R.Y., & Tzeng, S.C. (2006). Numerical research of natural convective heat transfer enhancement filled with nanofluids in rectangular enclosures. Int. Comm. Heat Mass Transfer.

[26] Corcione, M. (2011). Empirical correlating equations for predicting the effective thermal conductivity and dynamic viscosity of nanofluids. Energy Conversion and Management.

[27] Maïga, S.E.B., et al. (2005). Heat transfer behaviours of nanofluids in a uniformly heated tube. Superlattices and Microstructures.

[28] Sheikholeslami, M., & Ganji, D.D. (2015). Nanofluid convective heat transfer using semi analytical and numerical approaches. Journal of the Taiwan Institute of Chemical Engineers.

[29] Sheikholeslami, M., & Rokni, H.B. (2017). Simulation of nanofluid heat transfer in presence of magnetic field. International Journal of Heat and Mass Transfer.

[30] Jue, T.C. (2006). Analysis of combined thermal and magnetic convection ferrofluid flow in a cavity. International Communications in Heat and Mass Transfer.

[31] Devi, S.S.U., & Devi, S.P.A. (2016). Numerical investigation of three-dimensional hybrid Cu–Al2O3/water nanofluid flow over a stretching sheet with effecting Lorentz force subject to Newtonian heating. Canadian Journal of Physics.

[32] Tayebi, T., & Chamkha, A.J. (2020). Natural convection enhancement in a porous cavity with Al2O3–Cu/water hybrid nanofluid. Journal of Thermal Analysis and Calorimetry.

[33] Alawi, O.A., et al. (2020). Thermal conductivity and viscosity models of metallic oxides nanofluids. International Journal of Heat and Mass Transfer.

[34] Garandet, J.P., et al. (1992). Buoyancy driven convection in a rectangular enclosure with a transverse magnetic field. International Journal of Heat and Mass Transfer.

[35] Davidson, P.A. (2001). An introduction to magnetohydrodynamics. Cambridge University Press.

[36] Moreau, R. (1990). Magnetohydrodynamics. Kluwer Academic Publishers.

[37] Alchaar, S., et al. (1995). Natural convection heat transfer in a rectangular enclosure with a transverse magnetic field. Journal of Heat Transfer.

[38] Rudraiah, N., et al. (1995). Effect of a magnetic field on free convection in a rectangular enclosure. International Journal of Engineering Science.

[39] Yu, P.X., & Qiu, J.X. (2004). Numerical simulation of magnetohydrodynamic natural convection in a square enclosure. Numerical Heat Transfer, Part A: Applications.

[40] Grosan, T., et al. (2009). Magnetic field and internal heat generation effects on the free convection in a rectangular cavity filled with a porous medium. International Journal of Heat and Mass Transfer.

[41] Sheikholeslami, M., et al. (2013). Natural convection of nanofluids in an enclosure between a circular and a sinusoidal cylinder in the presence of magnetic field. International Communications in Heat and Mass Transfer.

[42] Ghasemi, B., et al. (2011). Magnetic field effect on natural convection in a nanofluid-filled square enclosure. International Journal of Thermal Sciences.

[43] Nield, D.A., & Bejan, A. (2013). Convection in porous media. Springer.

[44] Vafai, K. (2005). Handbook of porous media. CRC Press.

[45] Baytaş, A.C., & Pop, I. (2002). Free convection in a square porous cavity using a thermal nonequilibrium model. International Journal of Thermal Sciences.

[46] Chamkha, A.J., & Abu-Nada, E. (2012). Mixed convection flow in single- and double-lid driven square cavities filled with water–Al2O3 nanofluid. International Journal of Heat and Mass Transfer.

[47] Sheremet, M.A., et al. (2015). Natural convection in an inclined cavity filled with a porous medium saturated with a nanofluid. European Journal of Mechanics - B/Fluids.

[48] Grosan, T., & Pop, I. (2011). Thermosolutal natural convection in a square porous cavity under magnetic field. International Journal of Heat and Mass Transfer.

[49] Ali, A., Pan, K., Shah, M. A., Khan, N. Z., & Badshah, Z. (2024). Entropy impact on MHD nanofluid flow in an enclosure with corrugated wall and elliptical cylinder: Brinkmann–Forchheimer model and FEM analysis. *The European Physical Journal Plus*, *139*(8), 1-22.

[50] Ali, R., Imtiaz, R., Badshah, Z., Ali, A., & Hendy, A. S. (2025). Finite element analysis of natural convection and entropy generation under the influence of magnetic field in a wavy enclosure. *Physics of Fluids*, *37*(8).

[51] Mahian, O., et al. (2013). A review of entropy generation in nanofluid flow. International Journal of Heat and Mass Transfer.

© 2027 NSP
Natural Sciences Publishing Cor.

[52] Ali, A., Pan, K., Shah, M. A., Khan, N. Z., & Badshah, Z. (2025). Numerical study of natural convection heat transfer in a curve-shaped enclosure with MHD effects and hybrid nanofluids. *The European Physical Journal Plus*, *140*(1), 20.

[53] Bejan, A. (1996). Entropy generation minimization. CRC Press.

[54] Magherbi, M., et al. (2003). Entropy generation at the onset of natural convection. International Journal of Heat and Mass Transfer.

[55] Ilis, G.G., et al. (2008). Effect of aspect ratio on entropy generation in a rectangular cavity with differentially heated vertical walls. International Communications in Heat and Mass Transfer.

[56] Costa, V.A.F., et al. (2004). Natural convection in wavy enclosures.

[57] Lee, J.M., et al. (2012). Natural convection in a square enclosure with two hot inner cylinders. Numerical Heat Transfer, Part A: Applications.

[58] Roslan, R., et al. (2011). Natural convection in an enclosure containing a sinusoidally heated cylindrical source. International Communications in Heat and Mass Transfer.

[59] Mehrizi, A.A., et al. (2012). [Reference for wavy inner cylinder].

[60] Shah, M. A., Ali, A., Badshah, Z., Khan, F., Kallel, M., Alanazi, M. M., & Khan, M. I. (2025). Hydrothermal Characteristics with Entropy generation Impact on Brinkmann-Forchheimer MHD Nano-Fluid Model in a Corrugated Wall Cavity via Wavy cylinder. *Tribology International*, 110958.

[61] Tahir, N., Khan, N. Z., Abbasi, W. S., Ayaz, M., Ahmad, Z., & Alhmiedat, T. (2025). Numerical Investigation of Wake Dynamics and Flow Interference Effects on Fluid-Structure Interaction of Dual Side-by-Side Rectangular Cylinders: A Lattice Boltzmann Study. *Results in Engineering*, 107578.

[62] Timofeeva, E.V., et al. (2007). Particle shape effects on thermophysical properties of alumina nanofluids. Journal of Applied Physics.

[63] Prasher, R., et al. (2006). Effect of aggregation on thermal conduction in colloidal nanofluids. Applied Physics Letters.

[64] Buongiorno, J. (2006). Convective transport in nanofluids. Journal of Heat Transfer.; [65] Koo, J., & Kleinstreuer, C. (2004). A new thermal conductivity model for nanofluids. Journal of Nanoparticle Research.

[65] Duangthongsuk, W., & Wongwises, S. (2009). Measurement of temperature-dependent thermal conductivity and viscosity of TiO2-water nanofluids. Experimental Thermal and Fluid Science.

[66] Vajjha, R.S., & Das, D.K. (2009). Experimental determination of thermal conductivity of three nanofluids and development of new correlations. International Journal of Heat and Mass Transfer.

[67] Teamah, M.A., & El-Maghlany, W.M. (2010). Augmentation of natural convective heat transfer in square cavity by utilizing nanofluids in the presence of magnetic field and uniform heat generation/absorption. International Journal of Thermal Sciences.

[68] Teamah, M.A. (2008). Numerical simulation of double diffusive natural convection in rectangular enclosure in the presence of magnetic field and heat source. International Journal of Thermal Sciences.

[69] Mahmud, S., et al. (2003). Magnetohydrodynamic free convection and entropy generation in a square porous cavity. International Journal of Heat and Mass Transfer.

[70] Pirmohammadi, M., & Ghassemi, M. (2009). Effect of magnetic field on convection heat transfer inside a tilted square enclosure. International Communications in Heat and Mass Transfer.

[71] Mehryan, S.A.M., et al. (2017). Natural convection of magnetic hybrid nanofluid inside a double-porous medium using two-equation energy model. Journal of Molecular Liquids.

[72] Tasnim, S.H., & Collins, M.R. (2004). Entropy generation in a square enclosure with partial heating and cooling. Journal of Heat Transfer.

[73] Beckermann, C., et al. (1988). Natural convection in vertical enclosures containing simultaneously fluid and porous layers. Journal of Fluid Mechanics.

[74] Javed, T., et al. (2018). Numerical investigation of MHD natural convection in a nanofluid-filled incinerator-shaped porous enclosure. Journal of Thermal Analysis and Calorimetry.

[75] Khan, N. Z., Tahir, N., Shflot, A. S., & Malik, M. Y. (2025). Entropy generation and heat transfer in MHD free convection within l-shaped cavities: A computational and AI-based approach. *Results in Engineering*, *26*, 104659.

[76] Saeid, N.H. (2004). Natural convection in porous cavity with sinusoidal bottom wall temperature variation. International Communications in Heat and Mass Transfer.

[77] Mahian, O., et al. (2014). Entropy generation between two vertical cylinders in the presence of MHD flow subjected to constant wall temperature. International Communications in Heat and Mass Transfer.

[78] Varol, Y., et al. (2008). Entropy generation due to natural convection in non-uniformly heated porous isosceles triangular enclosures. Energy.

[79] Cho, C.C. (2018). Entropy generation of nanofluid convection in a heated porous microchannel under magnetic field. International Journal of Heat and Mass Transfer.

[80] Alsabery, A.I., et al. (2020). Entropy generation and natural convection flow of hybrid nanofluids in a partially divided wavy cavity including solid blocks. Energies.

[81] Z. Badshah et al., "Impact of variation in gap spacing and orientation of split baffles on thermodynamics optimization in naturally convective flow in corrugated enclosure," Numer. Heat Transf., Part A: Appl., 2024.

[82] Z. Badshah et al., "Numerical investigation of MHD natural convection in a hexagonal enclosure with heated corrugated cylinder," Eur. Phys. J. Plus, vol. 139, p. 709, 2024.

[83] Z. Badshah et al., "Enhanced natural convection and entropy generation in a porous crown cavity filled with copper nanoparticles under a horizontal magnetic field," Eur. Phys. J. Plus, vol. 139, p. 608, 2024.

[84] Z. Badshah et al., "Taming thermodynamic chaos and entropy generation study in MHD Al_2O_3-water nanofluid flow through corrugated porous media using Brinkman-Forchheimer model," Chaos, Solitons & Fractals, vol. 202, p. 117488, 2026.

© 2027 NSP
Natural Sciences Publishing Cor.

[85] D. Moher et al., "Preferred reporting items for systematic reviews and meta-analyses: The PRISMA statement," PLoS Med, vol. 6, no. 7, p. e1000097, 2009.

[86] B. Kitchenham and S. Charters, "Guidelines for performing systematic literature reviews in software engineering," EBSE Tech. Rep., EBSE-2007-01, 2007.

[87] H. Snyder, "Literature review as a research methodology: An overview and guidelines," J. Bus. Res., vol. 104, pp. 333-339, 2019.

[88] J. P. Higgins and S. Green, Eds., Cochrane handbook for systematic reviews of interventions. Wiley-Blackwell, 2011.

[89] Al_2O_3-water nanofluid flow through corrugated porous media using Brinkman-Forchheimer model," Chaos, Solitons & Fractals, vol. 202, p. 117488, 2026.

[90] D. Tranfield et al., "Towards a methodology for developing evidence-informed management knowledge by means of systematic review," Br. J. Manag., vol. 14, no. 3, pp. 207-222, 2003.

[91] J. C. Maxwell, A treatise on electricity and magnetism. Clarendon Press, 1873.

[92] P. Forchheimer, "Wasserbewegung durch boden," Z. Ver. Deutsch, Ing., vol. 45, pp. 1782-1788, 1901.

[93] A. Bejan, Convection heat transfer. John Wiley & Sons, 2013.

[94] A. Bejan, "Entropy generation minimization: The new thermodynamics of finite-size devices and finite-time processes," J. Appl. Phys., vol. 79, no. 3, pp. 1191-1218, 1996.

[95] M. Borenstein et al., Introduction to meta-analysis. John Wiley & Sons, 2021.

[96] M. A. Rosen and I. Dincer, "Exergy analysis of waste emissions," Int. J. Energy Res., vol. 23, no. 13, pp. 1153-1163, 1999.

© 2027 NSP
Natural Sciences Publishing Cor.